universität wien

MASTERARBEIT / MASTER'S THESIS

Titel der Masterarbeit / Title of the Master's Thesis

„Analysis of Actinides in Cryoconites"

verfasst von / submitted by

Maximilian Georg Bartmann, B.Sc.

angestrebter akademischer Grad / in partial fulfilment of the requirements for the degree of

Master of Science (M.Sc.)

Wien, 2017 / Vienna 2017

Studienkennzahl lt. Studienblatt / degree programme code as it appears on the student record sheet:	A 066 862
Studienrichtung lt. Studienblatt / degree programme as it appears on the student record sheet:	Masterstudium Chemie
Betreut von / Supervisor:	ao. Univ.-Prof. Mag. Dr. Gabriele Wallner

When the highest knowledge the deepest wisdom and the most open heart come together god appears

Acknowledgement

First of all I want to thank my supervisor, Ao. Univ.-Prof. Gabriele Wallner, for her great support and confidence in me during the hole work for this thesis.

I also want to thank the VERA institute and especially Dr. Karin Hain for her introduction and guidance during the AMS procedure.

My special thanks go to my colleagues Phillip Zima and Markus Brenner for the good times in the laboratory.

At last I want to thank my family for always giving me love and a save space when I needed it.

Tables of Contents

1.Introduction

The Institute of Inorganic Chemistry at the University of Vienna has a long and rich tradtition in the investigation of natural and anthropogenic radionuclides in environmental samples. Cryoconites are a new type of environmental samples which have never been investigated at the institute up till now. Therefore this thesis can be seen as starting point for a new research topic.

The samples for this thesis have been provided by the University of Salzburg which already investigated and published data for some anthropogenic nuclides in cryoconites (e.g. ^{137}Cs, ^{90}Sr, $^{239+240}$Pu). The extended possibility of Accelerator Mass Spectroscopy provided by the VERA Laboratory in Vienna allow investigations beyond the previous analysis as the measurements of the ^{240}Pu/^{239}Pu and ^{236}U/^{238}U atomic ratios. The characteristics of cryoconites being 'pure' fallout allow to search and detect neptunium and americium. Neptunium is of special interest due to the fact that there have been no reports for its occurrence in Austrian environmental samples yet.

In the following a short overview of the radionuclides of interest is given as well as a description of the investigated samples: cryoconites from an Alpine glacier in the south of Upper Austria.

1.1 Uranium

Uranium is one of the most abundant natural occurring actinides. It shares the characteristic of all actinides that only non-stable isotopes exist.[3] Four different isotopes of uranium can be found in the environment (Table 1.). The origin of the primordial isotopes ^{238}U and ^{235}U is the nucleosynthesis in the r-process of supernovae. During this process of high neutron flux ^{235}U and ^{238}U are formed and after explosion of the star became part of dust which formed the earth. Due to their long half-lives both can still be found in the environment today and are the starting points for two of the three natural decay chains. ^{234}U is formed during the decay of ^{238}U in the Uranium-Radium decay chain and is therefore a radiogenic nuclide.

Isotope	Half–life (a)	Abundance (w%)	Decay-mode	Energy
^{234}U	$2.455*10^5$	0.0055 %	α	4.775 MeV
^{235}U	$7.038*10^8$	0.7200 %	α	4.400 MeV
^{236}U	$2.342*10^7$	trace	α	4.494 MeV
^{238}U	$4.468*10^9$	99.2745 %	α	4.197 MeV

Table 1. Abundance and half-life of natural occurring Uranium isotopes [2][3]

1.1.1 ^{236}U

^{236}U with its half- life of $2{,}342*10^7$ years can be found in traces throughout the environment, although it is not part of any natural decay chain nor is any significant amount from the primordial processes left due to its rather short half- life compared to the earth's age . Its origin are the reactions

$$^1_0n + {}^{235}_{92}U \rightarrow [{}^{236}_{92}U] \rightarrow {}^{236}_{92}U + \gamma \qquad (\mathbf{1})$$

$$^1_0n + {}^{238}_{92}U \rightarrow [{}^{239}_{92}U] \rightarrow {}^{236}_{92}U + 3\,{}^1_0n \qquad (\mathbf{2})$$

$$^{240}_{94}Pu \rightarrow {}^{236}_{92}U + {}^4_2He \qquad (\mathbf{3})$$

1 and **2** are induced by neutrons which can be generated by the reaction of smaller nuclides ((α,n)-reactions), spontaneous fission of ^{238}U or anthropogenic activity like atomic bombs or nuclear power plants. Reaction **1** is also the most important one after detonation of uranium fission bombs. The cross section of the reaction {$\sigma[^{235}U(n,\gamma)]$ = 98 barn} is about $1/6$ of the cross section of the fission {$\sigma\,[^{235}U(n,f)]$ = 583 barn}. Reaction **2** is the dominant reaction for thermonuclear or fusion bombs due to the "tamper" of the bomb device which contains ^{238}U.[8]

3 is the alpha decay of ^{240}Pu which is also an anthropogenic nuclide but not considered a main source of ^{236}U due to its half-life of 6564 a [3] and its first appearance in the environment in the middle of the 20th century. The abundance of ^{236}U depends strongly on the specific sample, with values for $^{236}U/^{238}U$ ratios from 10^{-3} to 10^{-14} (Table 2.)

Source	$^{236}U/^{238}U$	Reference
Uranium ores	10^{-12} - 10^{-9}	[8]
Land surface	$3x10^{-14}$ (estimated)	[12]
Oceans	$1x10^{-14}$ - $1x10^{-13}$ (estimated)	[8]
Typical rocks in the uppermost 1km of earth`s surface	$1x10^{-14}$ - $5x10^{-14}$ (estimated)	[8]
Nuclear fuel	up to 10^{-2}	[10]
Environment around Chernobyl	up to 10^{-3}	[11]
Global Fallout	10^{-9} - 10^{-7}	[8]
Reprocessing plant (Sellafield)	10^{-5} - 10^{-6}	[9]

Table 2. $^{236}U/^{238}U$ ratios in different natural and anthropogenic samples

The significantly higher $^{236}U/^{238}U$ ratios on the land surface compared to an isolated environmental matrix like rocks in the uppermost 1km of earth`s surface can be explained with the high anthropogenic input of ^{236}U in the environment during the 20th century. 543 atmospheric nuclear detonations took place between the years 1945 and 1980, with a maximum between 1957 and 1963 (Figure 1).[8]

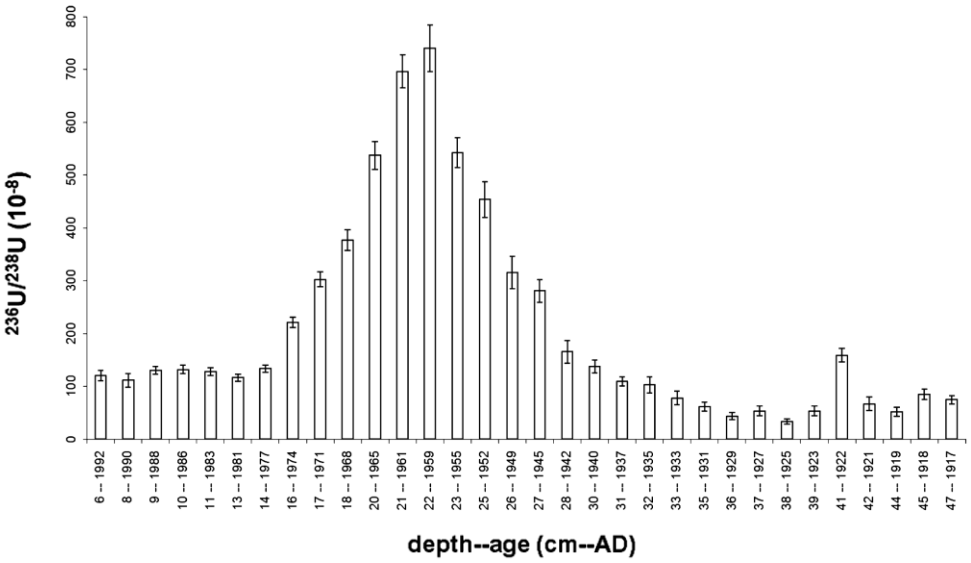

Figure 1. $^{236}U/^{238}U$ ratios in peat as function of depth and age. [8]

The estimates for the amount of ^{236}U in the environment produced during stratospheric atomic bomb tests range from 900-2100 kg. [8] Another source of anthropogenic ^{236}U is the burn-up of nuclear fuel in nuclear power plants. Discharge, reprocessing plants and accidents (Chernobyl) lead to a contamination of the environment.

The difference of several orders of magnitude between natural and anthropogenic $^{236}U/^{238}U$ ratios offer the possibility to use it as a tracer for anthropogenic nuclear activity. The highest natural ratio being 10^{-9}, ratios above this value indicate anthropogenic activity.

1.1.2 Chemical characteristics of Uranium

Atomic number (Z)	92
Block	f-block
Period	7
Element category	Actinide
Standard atomic weight	238.02891 u
Electron configuration	[Rn] $5f^3$ $6d^1$ $7s^2$
Oxidation states	+3,+4,+5,+6
Electronegativity	1.7

Table 3. Basic characteristics of Uranium [1]

U(0)

Refined Uranium is a slivery-white metal with a Mohs hardness of 6. Under oxygen atmosphere it gets coated by UO_3 and as a fine powder reacts pyrophoric. In general it is a very reactive metal and reacts with wide variety of elements and their compounds. In presence of conc. HNO_3 it gets passivated and with additional F^- ions it gets dissolved. Conc. HCl dissolves it, in non-oxidizing acids other than HCl it reacts very slowly. [1]

U(III)

In its lowest oxidation state uranium forms halogenoides UX_3 (X= F, Cl, Br, I) and UH_3. U^{+III} in aqueous solution is not stable and gets oxidized to U^{+IV}. [1]

U(IV)

U(IV) also forms halogenoides of the type UX_4. The oxide UO_2 is of basic character and crystallizes in the fluoride type. Aqueous solutions of U^{4+} have a green color and are slowly oxidized by air to UO_2^{2+}. [1]

U(V)

There are known halogenides of U(V) which disproportionate to U(IV) and U(VI) halogenoides. UO_2^+ is not stable in solutions and disproportionates to UO_2^{2+} and U^{4+}. [1]

U(VI)

U(VI) is the most stable oxidation state. The ion UO_2^{2+} or uranyl ion is the most common ion of all known uranium compounds. It is a linear molecule with possible multiple bonds between uranium and oxygen (Figure 2). [1][41]

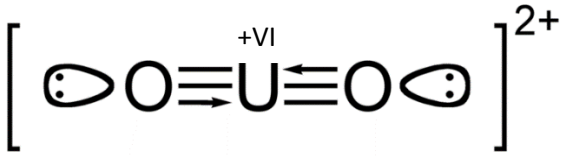

Figure 2. UO_2^{2+} Ion

The chemistry of the uranyl cation in water is highly complex, depending on many factors such as pH, uranium concentration, temperature and dissolved carbonate.[27] Figure 3. shows the influence of the pH on the complexation of the uranyl cation at 25 °C in water without carbonate or other anions. Starting from the solvent free UO_2^{2+} in aqueous solution at pH 2 with increasing pH species of the type $[(UO_2)_2(OH)_2]^{2+}$, $[(UO_2)_4(OH)_6]^{2+}$, $[(UO_2)_3(OH)_5]^+$ $[(UO_2)_4(OH)_7]^+$, and $[UO_2(OH)_2]$ occur. In alkaline solution, the hydroxide species of type, $[(UO_2)_3(OH)_8]^{2-}$ and $[UO_2(OH)_3]^-$ occur.

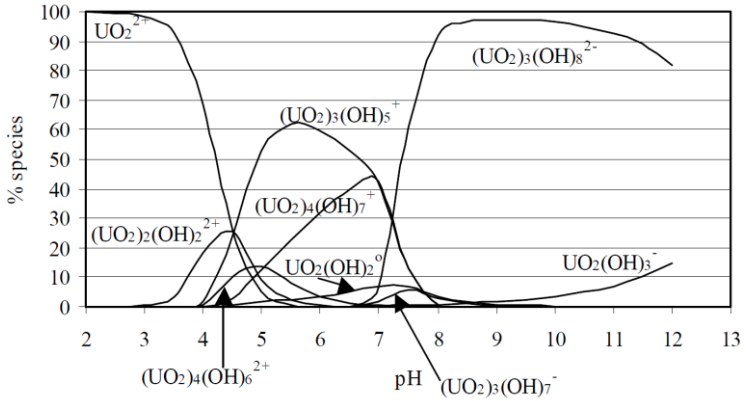

Figure 3. UO_2^{2+} in aqueous solution as a function of pH [33]

The effect of acids and their anions on the uranyl ion is strongly depending on the concentration of the respective anion. The two most important acids for this master thesis are nitric and hydrochloric acid. The data for hydrochloric acid shows the formation of $[UO_2Cl]^+$ from 0 to 0.3 M HCl, the formation of $[UO_2Cl_2]$ from 0.3 M to 0.9 M HCl, for concentrations higher than 0.9 M $[UO_2Cl_3]^-$ and higher than 3 M HCl $[UO_2Cl_4]^{2-}$. [5] A molecular dynamic simulation study shows that $[UO_2(OH_2)_5]^{2+}$ is the most abundant form at low acid concentration. With increasing acid concentration more water molecules are replaced with NO_3^-. The study found complexes of the form $[UO_2(OH_2)_4(NO_3)]+$, $[UO_2(OH_2)_3(NO_3)_2]$, and $[UO_2(OH_2)(NO_3)_3]^-$. [4][5]

1.2 Plutonium

Plutonium is a mainly anthropogenic actinide (trace amounts exist also naturally) with an electronic configuration $[Rn]5f^67s^2$. Its stable oxidation states in aqueous solutions are +III, +VI, +V and +VI. Due to the minor difference in the redoxpotential between these oxidation states, Plutonium can co-exist in several different states simultaneously. This fact makes the radiochemistry of Plutonium a very challenging task.[24][33] Table 4 shows the isotopes of the most concern.

Isotope	Half–life (a)	Decay-mode	Energy
^{238}Pu	87.74	α	5.499 MeV
^{239}Pu	2.411x10^4	α	5.157 MeV
^{240}Pu	6563	α	5.168 MeV
^{241}Pu	14.35	β	0.02 MeV
^{242}Pu	3.750x10^5	α	4.901 MeV

Table 4. Important anthropogenic isotopes of Plutonium in the environment[3]

Plutonium is used in fission bombs, atomic power plants or as energy supply for satellites. The two most important isotopes for those applications are ^{239}Pu and ^{238}Pu. The two important properties of ^{239}Pu are its rather easy production by irradiation of ^{238}U with neutrons (**4**) in nuclear power plants and its fissionability.

$$^{238}_{92}U(n,\gamma)^{239}_{92}U \xrightarrow{\beta^-(23.5\,\mathrm{min})} {}^{239}_{93}Np \xrightarrow{\beta^-(2.117\,\mathrm{d})} {}^{238}_{94}Pu \qquad (\mathbf{4})$$

^{238}Pu can be produced by the reaction of high energy neutrons with ^{238}U according to **5**.

$$^{238}_{92}U(n,2n)^{237}_{92}U \xrightarrow{\beta^-(6.75\,d)} {}^{237}_{93}Np(n,\gamma)^{238}_{93}Np \xrightarrow{\beta^-(2.117\,\mathrm{d})} {}^{238}_{94}Pu \qquad (\mathbf{5})$$

The origin of Pu isotopes can be determined by their $^{240}Pu/^{239}Pu$ ratio. The two ratios of the most concern for this thesis are the ratio for Chernobyl fallout ($^{240}Pu/^{239}Pu$: 0.4)[37] and global fallout in the northern hemisphere ($^{240}Pu/^{239}Pu$: 0.18) [36].

1.3 Americium and Neptunium

Americium and Neptunium are two anthropogenic actinides present at ultra-low levels in the environment, only occurring due to anthropogenic activity. Interesting isotopes for this thesis are ^{241}Am and ^{237}Np which are produced mainly via the reactions **6** and **7**. [24][38]

$$^{239}_{94}Pu(n,\gamma)^{240}_{94}Pu(n,\gamma)^{241}_{94}Pu \xrightarrow{\beta^-(14.35a)} {}^{241}_{95}Am \quad (\mathbf{6})$$

$$^{236}_{92}U(n,\gamma)^{237}_{92}U \xrightarrow{\beta^-(6.75d)} {}^{237}_{93}Np \quad (\mathbf{7})$$

^{241}Am and ^{237}Np are α-emitters with decay-energies of 5.486 and 4.790 MeV, and half-lives of 432.2 and $2.144*10^6$ a, respectively. Both nuclides are distributed in the environment through fallout from nuclear bomb tests and nuclear waste[35].

1.4 Cryoconites

Cryoconites (Greek: cold dust) are sediments with a black or grey color which accumulate on the surface of glaciers.[18] They have been first named by arctic explorer A.E Nordenskiöld in 1875 during his traveling over Greenland`s icecap.[14] Their coating makes glaciers look “dirty”, especially during summer. Due to their black color and therefore high absorption of light, cryoconites can induce a melting process that lead to so-called cryoconite holes. These cylindrical holes are filled with water and contain cryoconite on their bottom.[15] Their formation is depending on the movement, steepness and melting processes of the glacier.[17]

1.4.1 Components and formation of cryoconites

Investigation on cryoconites from Yala glacier in Nepal (Takeuchi et. al, 2001) showed their highly heterogenic character. The majority (~60%) of the volume are small dark colored granules with a diameter between 0.1 and 3.0 mm. Analysis of this particles with a microscope indicated that they are small aggregations of filamentous blue-green algae (Oscillatoriacean alga), cyanobacteria, bacteria, mineral particles and amorphous black matter. Figure 6 shows the cross section of dark colored granules.

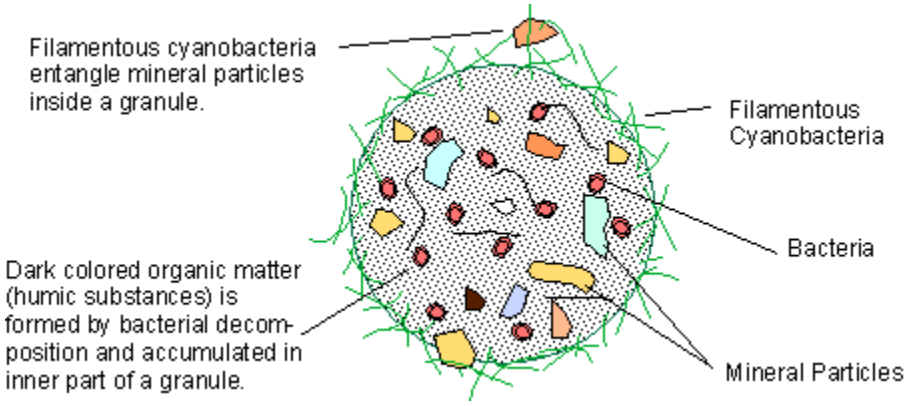

Figure 6. Structure of a cryoconite granule (cross section)[16]

In addition transparent and brown mineral particles (30-40% and 10-20% of the volume, respectively) and small organic particles (<1% of the volume) with diameter of <0.1mm median have been found. These particles, which can be seen as the origin of cryoconites are windblown material. The absence of typical cryoconite particles like the black granules in fresh windblown material suggests the formation of these particles on the glacier surface. The auto-fluorescent characteristics of algae pigments allowed the detection with fluorescent microscopy and suggested that the granule structure is formed by the filamentous blue-green algae. Analysis of the black granules and the brown/transparent particles showed significant higher amounts of carbon in the black granules, which indicates that the carbon amount was enriched due to photosynthesis of algae. Investigation on humic acid concentration found high amounts of humic acid in this material. The final conclusion of the investigation was, that algae are the source of the

shape of granules and organic matter (produced by photosynthesis) which gets decomposed by bacteria leading to dark humic substances. Although the glacier environment is a nutrition poor environment, the high density of living organism suggests that cryoconite granules are nutrient enriched microzones. An explanation of this observation is that the windblown material contains organic and inorganic nutrition needed for the development of microorganism. [17] In addition small animals like rotifer, tardigrade, insects and ice worm [15] have been found in cryoconite holes and show their important role in the ecosystem glacier.

1.4.2 Previous analyses of metals and radionuclides in cryoconites

The airborne sediments (described as brown and transparent particles in chapter 1.2.1) which are constantly deposited on glacier[18] are the origin of cryoconites. This airborne material transports also (anthropogenic) radionuclides to the glacier (fallout). In comparison to other environmental regions the galcier allows a soil- and therefore dilution-free sampling and therefore rather 'pure' fallout samples are obtained. So it is not surprising that two research groups (Tieber et al. 2009[18] and Lokas et al. 2016[17]) found high concentrations of radionuclides in cryoconites. The activity of artificial radionuclides has been described as "The highest in environmental media beside of bomb test sites".[18] This observation has been explained with the special behavior and characteristics of glaciers which can lead to an radionuclide enriched environment. One of the important facts is, that once deposited, windblown material is rather immobile compared to other environmental matrices.[18] Also the melting of the snow-layer in summer leads to a mixture of old layers of windblown material or cryoconites with newly deposited material. The resulting effect is an increasingly dense layer of cryoconite material which leads not only to high concentrations of radionuclides but also may cause accelerated glacier melting due to its high absorbance of sunlight and therefore heating up the glacier. [18]

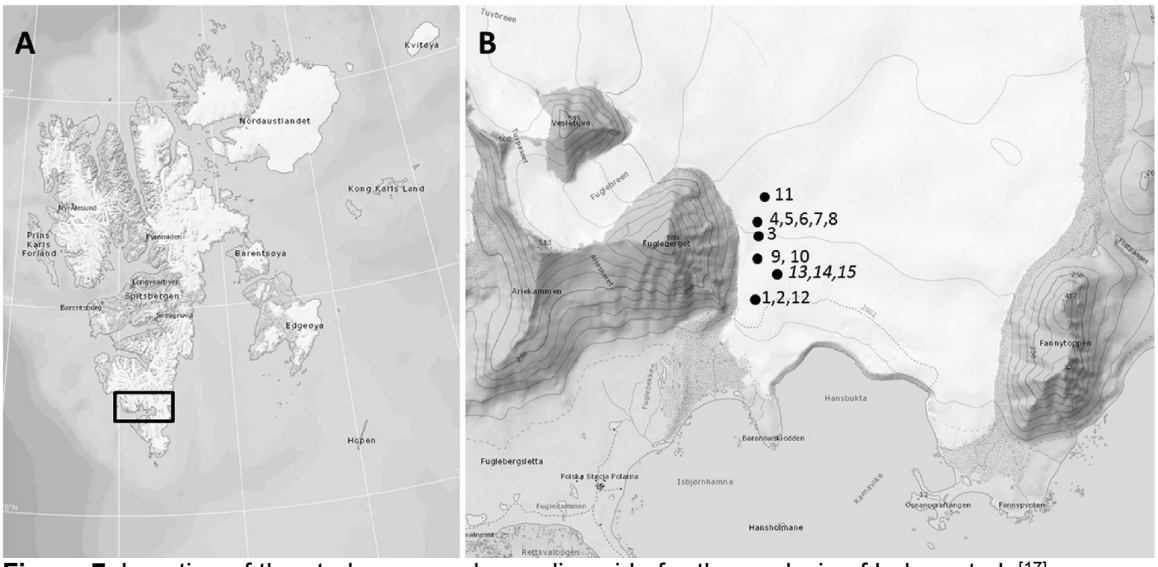

Figure 7. Location of the study area and sampling side for the analysis of Lokas et al. [17]

As mentioned above several groups have investigated the concentration of anthropogenic radionuclides in cryoconites on different glaciers. Lokas et al. reported research on cryoconites sampled from Svalbard archipelago (Figure 7.) in the European arctic with a spotlight on ^{238,239,240}Pu, ^{137}Cs, ^{90}Sr, ^{210}Pb and heavy metals (Table 5.).[17] The group of Tieber et al. from the University of Salzburg investigated samples from the Hallstätter and Schladminger glacier which are part of the Northern Calcareous Alps in Upper Austria (Figure 8.) regarding the nuclides ^{137}Cs, ^{134}Cs, ^{238}Pu,$^{239/240}$Pu, ^{90}Sr, ^{241}Am, ^{60}Co, ^{154}Eu, ^{207}Bi, and ^{125}Sb (Table 6.).[18] Both groups used gamma and alpha spectroscopy, as well as liquid scintillation counting for radiometric analysis. Flame atomic absorption spectroscopy and ICP-MS were used for heavy metal analysis.[17][18]

Sample No.	^{137}Cs (Bq/kg)	^{210}Pb (Bq/kg)	$^{239+240}$Pu (Bq/kg)	^{238}Pu (Bq/kg)	^{90}Sr (Bq/kg)	^{238}Pu/$^{239+240}$Pu	$^{239+240}$Pu/^{137}Cs	^{90}Sr/^{137}Cs	^{90}Sr/$^{239+240}$Pu	LOI (%)
1	89 ± 44	939 ± 153	1.65 ± 0.16	0.07 ± 0.03	80 ± 11	0.042 ± 0.022	0.019 ± 0.009	0.90 ± 0.13	48.5 ± 18.6	2
2	220 ± 46	2183 ± 156	2.42 ± 0.22	0.09 ± 0.03	53 ± 8	0.037 ± 0.011	0.011 ± 0.003	0.24 ± 0.06	21.9 ± 8.7	4
3	185 ± 40	1389 ± 127	5.61 ± 0.42	0.32 ± 0.05	79 ± 10	0.057 ± 0.011	0.030 ± 0.007	0.43 ± 0.11	14.1 ± 5.1	8
4	178 ± 49	1934 ± 169	4.89 ± 0.38	0.32 ± 0.06	78 ± 10	0.065 ± 0.014	0.028 ± 0.008	0.44 ± 0.13	16.0 ± 5.9	6
5	128 ± 36	2203 ± 151	3.40 ± 0.40	0.21 ± 0.07	101 ± 13	0.062 ± 0.021	0.027 ± 0.008	0.79 ± 0.24	29.7 ± 11.2	6
6	262 ± 66	2412 ± 207	7.35 ± 0.59	0.27 ± 0.02	51 ± 8	0.037 ± 0.004	0.028 ± 0.007	0.19 ± 0.06	6.9 ± 2.8	10
7	635 ± 85	3039 ± 185	10.49 ± 0.74	0.57 ± 0.09	70 ± 8	0.054 ± 0.009	0.017 ± 0.003	0.11 ± 0.02	6.7 ± 2.3	11
8	539 ± 74	4557 ± 255	11.14 ± 0.87	0.98 ± 0.15	58 ± 9	0.088 ± 0.015	0.021 ± 0.003	0.11 ± 0.02	5.2 ± 2.1	14
9	782 ± 99	2926 ± 164	16.62 ± 1.21	1.27 ± 0.17	89 ± 13	0.077 ± 0.012	0.021 ± 0.003	0.11 ± 0.02	5.4 ± 2.1	4
10	303 ± 49	1298 ± 112	7.39 ± 0.53	0.87 ± 0.11	59 ± 9	0.118 ± 0.017	0.024 ± 0.004	0.19 ± 0.04	8.0 ± 3.2	10
11	573 ± 89	2039 ± 105	10.18 ± 0.65	0.53 ± 0.04	22 ± 3	0.052 ± 0.005	0.018 ± 0.003	0.04 ± 0.01	2.2 ± 0.8	6
12	678 ± 91	2265 ± 141	10.65 ± 0.74	0.72 ± 0.08	24 ± 2	0.068 ± 0.009	0.016 ± 0.002	0.04 ± 0.01	2.3 ± 0.7	n.m.
13	235 ± 33	2185 ± 115	6.07 ± 0.40	0.24 ± 0.02	15 ± 2	0.040 ± 0.004	0.026 ± 0.004	0.06 ± 0.01	2.5 ± 0.9	6
14	191 ± 31	3675 ± 195	2.50 ± 0.20	0.18 ± 0.03	24 ± 4	0.070 ± 0.014	0.013 ± 0.002	0.13 ± 0.03	9.6 ± 4.0	13
15	349 ± 46	1975 ± 104	6.53 ± 0.48	0.66 ± 0.08	49 ± 5	0.101 ± 0.014	0.019 ± 0.003	0.14 ± 0.02	7.5 ± 2.5	7
Min	**89 ± 44**	**939 ± 153**	**1.65 ± 0.16**	**0.07 ± 0.03**	**15 ± 2**	**0.037 ± 0.004**	**0.011 ± 0.003**	**0.04 ± 0.01**	**2.2 ± 0.8**	
max	**678 ± 91**	**4557 ± 255**	**16.62 ± 1.21**	**1.27 ± 0.17**	**101 ± 13**	**0.118 ± 0017**	**0.030 ± 0.007**	**0.90 ± 0.13**	**48.5 ± 18.6**	
Mean	**356 ± 58**	**2335 ± 156**	**7.13 ± 0.53**	**0.49 ± 0.07**	**57 ± 8**	**0.064 ± 0.012**	**0.021 ± 0.05**	**0.26 ± 0.06**	**12.4 ± 4.7**	
IAEA-447[a]	431 ± 19	413 ± 39	5.70 ± 0.43	0.18 ± 0.03	4.48 ± 0.45					
Certyfied values	425 ± 10	424 ± 20	5.3 ± 0.16	0.15 ± 0.015	5.0 ± 0.3					

Table 5. Results of the investigation of Lokos et al. [17]

The main findings of the investigation of the samples of Svalbard archipelago are:

- High activity of anthropogenic radionuclides
- Comparing ^{238}Pu/$^{239+240}$Pu and $^{239+240}$Pu/^{137}Cs ratios with data for global fallout lead to the suggestion that there is an addition source for ^{238}Pu and ^{137}Cs
- ^{90}Sr/^{137}Cs and ^{90}Sr/$^{239+240}$Pu activity ratios are much lower than in global fallout because strontium can be removed from the cryoconites due to its high solubility in water
- Heavy metals do not origin exclusively from natural sources but also from anthropogenic sources

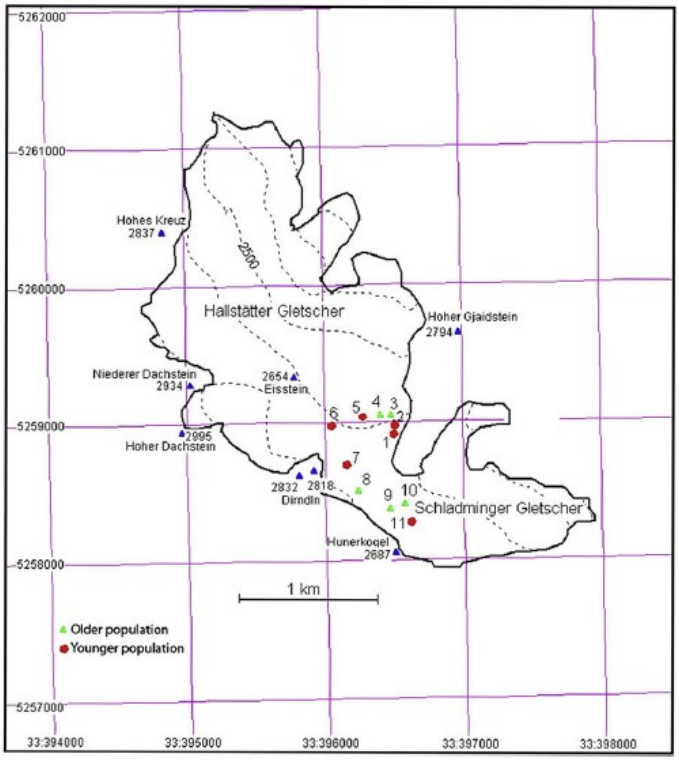

Figure 8. Location of the study area and sampling side for the analysis of Tiber et al. [18]

Sample	^{134}Cs		^{137}Cs		^{241}Am		^{60}Co		^{154}Eu		^{207}Bi		$^{239+240}$Pu		^{238}Pu		^{90}Sr	
[Bq/kg]	[Bq/kg]	s	[Bq/kg]	s	[Bq/kg]	s	[Bq/kg]	s	[Bq/kg]	s	[Bq/kg]	s	[Bq/kg]	s	[Bq/kg]	s	[Bq/kg]	s
Cryo. 1	13.1	1.3	14 350	1003	<2.2		<0.5		<1.7		<1.4		3.2	0.3	0.31	0.07	27.3	4.1
Cryo. 2	115.5	17.3	120 267	17 330	<6.9		2.4	0.5	<3.4		<4.6		11.9	0.5	1.62	0.12	110.1	16.5
Cryo. 3	27.8	2.1	31 509	1948	78.8	5.9	0.7	0.2	<1.3		22.2	1.3	164.6	6.6	4.73	0.38	115.6	17.3
Cryo. 4	35.5	2.7	41 161	2545	93.6	7.1	<0.5		<1.4		27.5	1.7	152.8	6.1	5.02	0.39	133.2	20.0
Cryo. 5	42.5	3.5	45 571	3187	<3.7		1.3	0.2	0.6	0.2	<2.6		3.7	0.3	0.66	0.10	71.8	10.8
Cryo. 6	<4.6		1744	150	<3.9		<2.0		<6.8		<1.4		1.6	0.2	0.11	0.04	246.2	36.9
Cryo. 7	137.9	8.6	140 051	8460	<6.4		2.4	0.4	6.7	0.2	<13.2		9.3	0.6	1.32	0.15	197.1	29.6
Cryo. 8	10.6	2.2	17 083	2462	82.2	14.6	<1.3		<3.7		20.6	3.2	118.5	7.3	4.31	0.61	102.6	15.4
Cryo. 9	18.4	1.67	24 793	1901	93.3	9.4	<0.5		<1.5		21.2	1.6	196.1	7.5	5.57	0.40	140.4	21.1
Cryo. 10	18.3	3.1	31 125	2558	74.4	8.6	<2.2		<6.6		21.8	2.7	197.9	7.7	6.27	0.46	163.6	24.4
Cryo. 11	95.3	7.1	95 446	7317	<4.9		1.1	0.3	3.7	0.9	<7.0		16.1	1.0	1.04	0.15	64.0	9.6

Table 6. Results of the investigation of Tieber et al.[18]

The main findings of the analysis from the samples the Northern Calcareous Alps are:

- High activity of anthropogenic radionuclides
- Analysis of ^{134}Cs/^{137}Cs and ^{238}Pu/$^{239+240}$Pu activity ratios shows a mixing process of fallout from nuclear weapons testing and Chernobyl fallout taking place
- Strontium depletion takes place and is manifested in element ratios

The comparison of data from Austria and the Arctic showed differences in the activity of ^{238,239,240}Pu, ^{137}Cs and ^{90}Sr, which were significantly higher in the samples from the glacier

in Upper Austria. This can be explained with the spatial proximity of Austria with regard to the Chernobyl accident, when high amounts of $^{238,239,240}Pu$ (4,6 * 10^{13} Bq)[19], ^{137}Cs (8,5*10^{16} Bq)[19], ^{90}Sr (1,0*10^{16} Bq)[19] were released.[17]

2. Main Task of this master thesis

The fact that up till now there is no data for uranium in cryoconites available and the possibility of working with Acclerator Mass Spectroscopy (AMS) (Chapter 3.1.2), give the opportunity to be among the first presenting data on this topic. The VERA Laboratory in Vienna is one of the few facilities worldwide that allow the measuring of ^{236}U for concentrations that occur in the enivronment. Due to the unique formation process of ^{236}U, which is only possible in a matrix of high neutron flux like nuclear bombs and the fact that cryoconites contain very high amounts of accumulated fallout, the activity of ^{236}U and the $^{236}U/^{238}U$ ratios should be among the highest to be found in nature. Given the fact that $^{236}U/^{238}U$ ratios in global fallout range from 10^{-7} to 10^{-9}, values of this order of magnitude or even higher are to be expected.

The main task of this thesis is

- First quantification of ^{236}U and $^{236}U/^{238}U$ atomic ratios in the cryoconite samples Cryo.3, Cryo.7, Cryo.9 and Cryo. 11 from the Hallstätter and Schladming glacier which have already been investigated in [18]
- The reproduction of the data for the already investigated species ^{137}Cs, ^{238}Pu and $^{239+240}Pu$, with a spotlight on the $^{240}Pu/^{239}Pu$ atomic ratios which are only accessible by AMS measurement

In addition to the main task the thesis allows

- The analysis of ^{241}Am and the $^{243}Am/^{241}Am$ ratios with AMS and alpha spectroscopy
- The first step for detection of ^{237}Np (without a specific method), which has not been measured in samples from Austria yet
- To investigate the possibility of using a different and cheaper ion exchange resin compared to [18]

3. Experimental procedure

The samples were collected in October 2006 by H. Lettner and his group from the Institute of Physics and Biophysics, University of Salzburg, Austria. Samples were dried at 105°C until constant weight.

The activity concentration of ^{137}Cs was measured by γ-spectrometry; this works without any sample-pretreatment. However, for the determination of the activity concentrations of uranium, thorium or plutonium isotopes α-spectroscopy and its corresponding strenuous sample preparation was necessary. Also for AMS measurements the separation of different nuclide fractions was needed. In the following chapters the analytical methods as well as the chemical sample procedures are described.

3.1 Applied analytical methodes

3.1.1. Alpha spectroscopy

In this master thesis an alpha spectrometer from Canberra was used. The Canberra Model 7401 with a semiconductor detector in which alpha particles create electron hole-pairs (counting efficiency for alpha particles ~ 0.3). The amount of generated electron hole-pairs is directly proportional to the energy of the alpha particle. This allows the identification and quantification of the respective α-emitters. Due to the short range of alpha particles in matter, the source preparation for this method is time consuming. For the measurement of actinides a co-precipitation with NdF_3 and filtration through a membrane with small pore-size is applied.[20] With this procedure a NdF_3 layer of about 10µm thickness is formed. The measurement is done in an evacuated chamber. The advantage of this technique is the low background as well as high selectivity regarding other types of radiation.[24] Although the energy resolution is very good it is not possible to distinguish between the alpha particles of some isotopes. ^{235}U alpha particles (4.395, 4.364 keV)[3] and ^{236}U alpha particles (4.494, 4.445 keV)[3] cannot be separated in the spectrum (Figure 9.) and therefore an additional technique is needed.

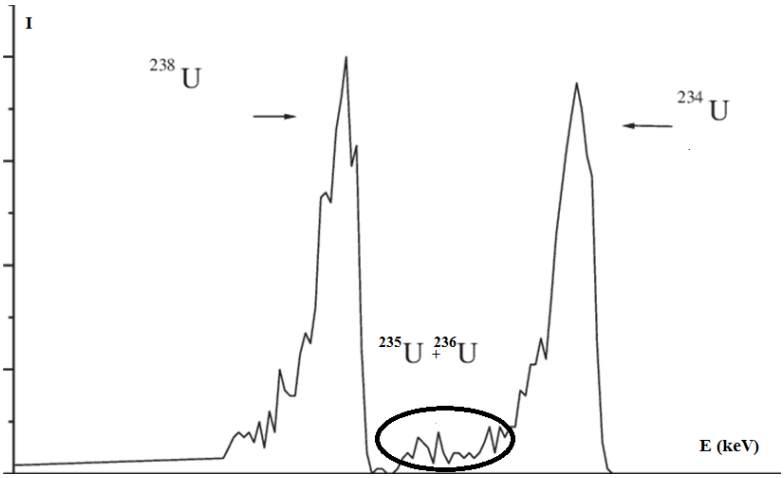

Figure 9. Alpha spectrum of uranium, showing the position of the isotope peaks

3.1.2 Accelerator Mass Spectroscopy

As mentioned in chapter 3.1.1, alpha spectroscopy does not provide a high enough resolution to separate ^{235}U and ^{236}U alpha particles. Accelerator Mass Spectroscopy (AMS) is one of the few techniques available for the separation and detection of natural $^{236}U/^{238}U$ ratios.[31] The detection limit for normal mass spectroscopy for $^{236}U/^{238}U$ is around 10^{-10}.[32] It is one of the most sensitive ways to measure radionuclide ratios.[30] By combining mass spectroscopy with a tandem accelerator (0.5 – 15 MeV), the detection of small amounts of atoms (10^5 – 10^8) or low isotope ratios (10^{-10} – 10^{-16}) can be achieved.[25]

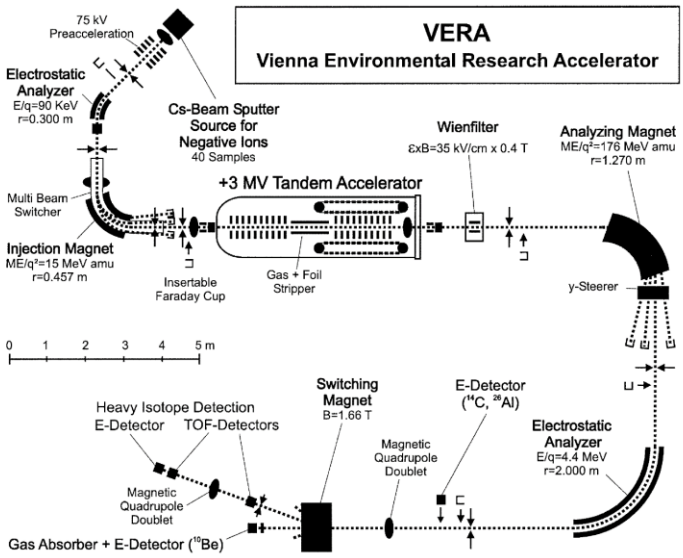

Figure 10. Schematic layout of the VERA facility [26]

The basic concept of Accelerator Mass Spectroscopy is the production of negative ions by cesium sputtering, which then get mass-selected by electrostatic and magnetic fields. After injection into the tandem accelerator, the ions get 'stripped' by argon (mbar range); this step destroys molecule ions and allows a second acceleration of the now positively charged ions with the same energy, resulting in particle energies of several MeV. After the acceleration a second analyzing magnet removes molecule break-up products. An electrostatic analyzer can bend heaviest elements with charge +V. Finally the atoms get detected by an appropriate particle detector.[25] This set-up is shown in the schematic layout in Figure 10.

The shown set-up allows the detection of $^{236}U/^{238}U$ ratios down to 10^{-11} and below depending on the setup and the available blank [25], which should be more than enough for the measurement of the $^{236}U/^{238}U$ in the Alpine cryoconite sample, given the expected high amount of ^{236}U. The parameters for the measurement of ^{236} U are given in Table 8.

Trace isotope	^{236}U
Target material	U_xO_y
Injection energy	57 keV
Injected ion	$^{236}U^{16}O^-$
Terminal voltage	3.0 MV
Analyzed ion	$^{236}U^{5+}$
Reference ions	$^{238}U^{5+}$
Typ. neg. Ion current (of reference species)	50 nA ($^{238}U^{16}O^-$)
Stripping yield[b]	5%
Machine background[c]	$\ll 6 \times 10^{-11}$
Detector efficiency[d]	20%
Total efficiency[e]	
Typ. Precision[f]	5%
Targets measured[h]	<10

[b] Ratio of analyzed reference ion to injected reference ion, including ion optical losses.
[c] Quoted for the ratio of trace to reference isotope. The chemistry blank will be higher.
[d] Measured as the fraction of analyzed ions observed in the final detector.
[e] Measured as counts in detector per total number of atoms in sputter target.
[f] For the ratio of trace to reference isotope in a sample significantly above the background and the efficiency limit.
[h] Between 9/2001 and 8/2002 incl. standards.

Table 7. Parameters for the measurement of ^{236}U at the VERA institute (modified table) [26]

With the measured $^{236}U/^{238}U$ ratios (AMS) and the known quantity of ^{238}U (alpha spectroscopy), calculation of the ^{236}U activity concentration is possible for all samples.

3.1.3 Gamma spectroscopy

The detection of radionuclides via their emitted gamma-rays is a frequently used technique with access to many radionuclides. The most common method is the use of a liquid nitrogen cooled (to eliminate electrical noise) high purity germanium crystal (HPGe) which offer the best compromise between resolution and efficiency.[28][29] Working with the same principle as alpha spectroscopy, gamma rays create electron-hole pairs in a semiconductor detector which can be quantified and give information about the energy of the gamma ray. The gamma spectrometer used for this work is the model GX8021/S from Canberra. A sample mass of 0.2 g was placed in the tip of an 1.5 mL Eppendorf® vial and in order to simulate a point source, samples were placed ~ 7cm above the HPGe detector.

3.2 Chemical methodes

The applied analytical methodes Alpha Spectroscopy and Accelerator Mass Spectroscopy (Chapter 3.1.1-3.1.2) require specific chemical and physical sample properties to allow correct measurements. To achieve these properties, several steps of sample preparation are necessary. This procedure can be distinguished in three parts: pretreatment of the samples with acids, separation of the actinides and precipitation of the α-source.

As mentioned in chapter 1.2.1 cryoconites contain many organic substances which can form complexes with actinides [20] and lead to insoluble precipitate during the preparation. Therefore decomposition of organic material is necessary. Cryoconites are particles of different size, which enclose a wide variety of different materials (Chapter 1.2.1). To ensure the dissolution of all actinides, repeated evaporating with HNO_3 and HCl mixed with H_3BO_3 have to be carried out according to [18].

The separation of actinides via ion exchange requires actinide complexes with specific ions. In some steps of the process, only one sort of anion is allowed and all other anions have to be removed from the sample. Repeated evaporating with the concentrated acid of the desired anion, removes other anions.

Separation of the actinides is done with the anion exchange resin DOWEX® 1X2 with a particle size of 100-200 mesh. This high-molecular compound of polymerized styrene with copolymer divinylbenzen contains covalent bound $R\text{-}[N(CH_3)_3]^+$ groups (Figure 11.). The description 1X2 indicates the crosslinking, which in this case is 2%.[22]

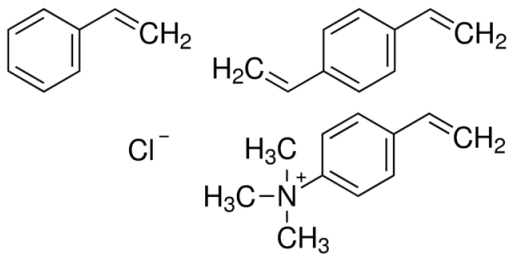

Figure 11. DOWEX® 1X2 resin chloride form [22]

Depending on the used acid and the concentration, actinides form different complexes in aqueous solutions (Chapter 1.2.2). The separation of actinides is possible due to the different absorption of these complexes on the resin. [23] In case of uranium the complex $[UO_2Cl_4]^{2-}$ is absorbed by exchanging with a chloride ion. For this application the resin is conditioned with 8M HCl. Rinsing with 0.1 M HCl changes the amount of chloride ions complexing the UO_2^+ and leads to the formation of $[UO_2Cl]^+$ (Chapter 1.1.2). The now cationic complex gets eluted from the column.

The measurement of alpha-particles requires a very thin precipitate (Chapter 3.1.1). Therefore co-precipitation with a small amount of NdF_3 (thickness of the layer<10 µm)[20] is performed after the separation. For this precipitation uranium has to be converted to +IV with $TiCl_3$. The precipitate is filtered off, washed and dried, and then measured by alpha spectroscopy.

The sample preparation for the AMS measurement was done by dissolving the NdF_3 in conc. HNO_3 and adding 1mL of pre-nuclear Fe^{3+} solution (2mg/mL) . The actinides were then co-precipitated with $Fe(OH)_3$ by adding conc. NH_3. The samples were dried and the $Fe(OH)_3$ was calcined at 800°C for 4 h. This ensures the oxidation to Fe_2O_3. This step is necessary to remove hydrogen atoms from the samples which can lead to hydride and hydroxide adducts during the measurement resulting in wrong results (as an example $^{238}UH^{+4}$ with a mass of 239 would be detected as $^{239}Pu^{+4}$).

3.3 Practical Procedure

The two main isotope fractions of interest were the uranium and plutonium fractions and therefore we used an approved protocol for their separation. It started with the Pu separation and Uranium was found in the washing solution of the Pu-column; in the next step the (usually discarded) Thorium fraction was eluted. In order to get an idea where the americium and neptunium fractions end up and find eventually misled U and Pu we also measured the thorium fraction as well as the washing solution of the uranium column (X-fraction).

To minimize cross contamination all glassware was washed with 7.2 M HNO_3 after each separation.

Plutonium

The samples were weighted and 10 µl ^{242}Pu spike (14.4 mBq/10 µl) and 10 µl ^{232}U spike (in radioactive equilibrium with ^{228}Th) (17.7 ± 0.9 mBq /10 µl) were added (not used for the samples that were measured with AMS due to possible interference during the AMS procedure). Samples were evaporated 3x with 10 mL suprapure® conc. HNO_3, 3x 10 mL suprapure® conc. HCl saturated with H_3BO_3 (800 mg / 30 mL, to ensure chemical digestion of silicates[13][18]) and again 3x with 10 mL conc. HNO_3 to ensure all Pu species in the oxidation state +IV [18]. The residue was dissolved in 20 mL 7.2 M HNO_3 and filtered off. The filtrate was loaded on a DOWEX® column (conditioned with 7.2 M HNO_3) and was washed with 2x 15 mL 7.2 M HNO_3. The eluate from the loading and the washing solution are combined and stored for the separation of uranium (U fraction). The column was then washed with 2x 15 suprapure® mL conc. HCl to eluate Thorium. This solution was stored for further analysis (defined as Th fraction). Plutonium was eluted with 50 mL 0.36 M HCl – 0.018 M HF in a beaker filled with 5 mL suprapure® conc. HNO_3 (to avoid plutonium polymerization and adsorption on beaker walls). The solution was evaporated to dryness and evaporated with 3x 5 mL suprapure® conc. HNO_3 + 2mL H_2O_2 (destroys resin particles and fluoride) and 3x 5 mL suprapure® conc. HCl. The residue was dissolved in 2 mL + 2x 1 mL 1M HCl. 100 µl 0.5 mg/mL Nd^{3+} solution and 0.5 mL conc. HF was added to obtain the NdF_3 precipitate for alpha spectroscopy. After 30 min the precipitate was filtered through a cellulose nitrate membrane filter (Whatman®, 0.1 µm pore size) which had been

washed with 4 mL NdF_3 (10mL 0.5 mg/mL Nd^{3+} Solution + 455 mL 1M HCl + 40 mL 48 % HF) solution before. The precipitate was washed with 2 mL 0.58 M HF and 2 mL H_2O, dried and then measured by alpha spectroscopy.

The procedure was validated by measuring the standard material IAEA-0375 (Radionuclides in Soil).

Uranium

The uranium fraction of 4.1 was evaporated to dryness and then evaporated with 3x with 5mL suprapure® conc. HCl to obtain the negatively charged chlorid uranium complex. The residue was dissolved in 80 mL 8 M HCl and then also loaded on a DOWEX® column (conditioned with 8 M HCl) and washed with 2x 25 mL 8 M HCl. The eluate from the loading and the washing solution were combined and stored for further analysis (defined as X fraction). The uranium was eluted with 2x 40 mL 0.1 M HCl and evaporated to dryness. The residue was evaporated with 3x with 5mL suprapure® conc. HNO_3 + 2mL H_2O_2 (destroys resin particles) and 3x with 5 mL suprapure® conc. HCl. The resulting residue was dissolved in 2 mL + 2x 1mL 1M HCl. 100 µl 0.5 mg / mL Nd^{3+} solution was added. $TiCl_3$ was added until the color of the solution was purple (indicating U^{+IV}). Usually the amount was between 10 and 17 drops (0.5 – 0.8 mL). The reduced uranium was co-precipitated with NdF_3 by adding 0.5 mL conc. HF. After 30 min the solution was filtered through a cellulose nitrate membrane filter (Whatman®, 0.1 µm pore size) which had been washed before with 4 mL NdF_3 (10mL 0.5 mg/mL Nd^{3+} Solution + 455 mL 1M HCl + 40 mL 48 % HF) solution. The precipitate was washed with 2 mL 0.58 M HF and 2 mL H_2O, dried and then measured by alpha spectroscopy.

The procedure was validated by measuring different in-house uranium standards.

Thorium

The Th fraction was evaporated to dryness and then evaporated with 3x with 5 mL suprapure® conc. HNO_3 + 2 mL H_2O_2 (destroys resin particles) and 3x with 5 mL suprapure® conc. HCl. The residue was dissolved in 2 mL + 2x 1mL 1M HCl and 100 µl 0.5 mg / mL Nd^{3+} solution was added. Co-precipitation was done by adding 0.5 mL conc. HF acid. After 30 min the solution was filtered through a cellulose nitrate membrane filter

(Whatman®, 0.1 µm pore size) which had been washed with 4 mL NdF_3 (10mL 0.5 mg/mL Nd^{3+} Solution + 455 mL 1M HCl + 40 mL 48 % HF) solution. The precipitate was washed with 2 mL 0.58 M HF and 2 mL H_2O, dried and then measured by alpha spectroscopy.

X- fraction

The analysis of the eluat from the loading and washing step of the column in 4.2 (uranium) was done to check for any nuclides having slipped through the hole procedure. The solution was evaporated to dryness and then evaporated with 3x with 5 mL suprapure® conc. HNO_3 + 2 mL H_2O_2 (destroys resin particles) and 3x with 5 mL suprapure® conc. HCl. The residue was dissolved in 2 mL + 2x 1mL 1M HCl and 100 µl 0.5 mg / mL Nd^{3+} solution was added. 10 drops of $TiCl_3$ was added. This was done to ensure the reduction of eventually still present uranium that was not captured by the resin. Co-precipitation was done by adding 0.5 mL conc. HF acid. After 30 min the solution was filtered through a cellulose nitrate membrane filter (Whatman®, 0.1 µm pore size) which had been washed with 4 mL NdF_3 (10mL 0.5 mg/mL Nd^{3+} Solution + 455 mL 1M HCl + 40 mL 48 % HF) solution. The precipitate was washed with 2 mL 0.58 M HF and 2 mL H_2O, dried and then measured by alpha spectroscopy.

Caesium-137

0.2 g sample was weighted into a 1.5 mL Eppendorf Safe-Lock Tube® and placed 7 cm above the gamma detector of the spectrometer described in chapter 3.1.3. and measured until 1000 counts were detected. A Reference from an in-house standard with an activity of 26764 Bq (Jan. 2107) was used to ensure correct data (Chapter 9.1).

AMS sample preparation

The cellulose nitrate membrane filter (Whatman®, 0.1 µm pore size) were cut in half. One part was used for the AMS procedure, the other one was stored for further investigation by other students. The filters were placed in a plastic tube filled with 5 mL conc. HNO_3 to dissolve the NdF_3 precipitate. After 10 min the filter was removed and 10 mL H_2O was added. 1mL of a prenuclear Fe^{3+} solution (2mg/mL) and 5 mL NH_3 were added to allow the formation of $Fe(OH)_3$. The samples were shaken and then centrifuged. The solution was discarded and the precipitate washed with 5 mL H_2O (500 mL H_2O + 3 drops conc.

NH_3), centrifuged again and the precipitate transferred to quartz vials. Calcination was done in an oven at 800°C for 4 h. The Fe_2O_3 was pressed in aluminum pins and measured by AMS.

The presence of U in the Pu fractions of Cryo.7 and Cryo.11 (found by Alpha Spectroscopy) made an additional cleaning step necessary to allow correct measurement of Plutonium by AMS procedure. For this purpose the precipitates were dissolved in 7.2 mL 8 M HNO_3 and passed through a UTEVA® resin conditioned in 8 M HNO_3. Here the uranium stays on the UTEVA®, while plutonium passes through the column (6.8 mL H_2O instead of 10 mL was added to the cleaned solutions to ensure the same concentration of acid).

4. Results

As described in chapter 2. the samples used for this master thesis are the samples already investigated by the group of Tieber et al.[18] For this master thesis the samples described as Cryo.3, 7, 9, and 11 (Table 8.) were analyzed with the preparation and measuring methodes described in chapter 3. These samples were selected because of their representation of the variablity of the activity concentrations (Table 8.).

In a first attempt the samples were measured with gamma spectroscopy (^{137}Cs) and then preparation was done without any spikes for the measurement by alpha spectroscopy and AMS (Chapter 3.3). The absence of spikes ensured the identification of all nuclides present in the samples and gave information about the expected number of atoms which is important for the AMS procedure. Due to to absence of any spike, quantification of the true activity is not possible. Therfore the results for the samples without spike are called 'estimated'. Pretreatment with acids (Chapter 3.2) for the unspiked procedure of Cryo 3. was done without H_3BO_3 to estimate the amount of actinides which are enclosed in silicates (Comparison of Pu data from [18] with the recent results).

In a second attempt, sample preparation was done with spike and samples were measured by alpha spectroscopy. The procedure for the spiked Cryo 3. was done differently than the others and therefore X fraction and Th fraction are not present. Instead a residue fraction was measured.

As a reference for $^{237}Np/^{239}Pu$ and $^{240}Pu/^{239}Pu$ ratios an IAEA (International Atomic Energy Agency) standard (IAEA 0375 Radionuclides in soil) was measured by AMS.

Radioactive background was checked with a blank procedure.

4.1 Sample preparation without spike (for AMS measurement)

4.1.1 Cryo. 3

Nuclide	Bq/kg estimated	Ratio	Comment
^{238}U	14.4 ± 0.4 1.0 ± 0.1	-	U fraction X fraction
$^{236}U/^{238}U$	-	8.03E-06 ± 6.50E-08 9.22E-06 ± 3.30E-07	U fraction X fraction
^{234}U	16.8 ± 0.5 1.6 ± 0.1	-	U fraction X fraction
$^{234}U/^{238}U$	-	5,36E-05 6,62E-05	U fraction X fraction
^{232}U	0.8 ± 0.1 9.4 ± 0.4	-	U fraction X fraction
$^{239+240}Pu$	121.8 ± 2.3	--	Pu fraction
$^{240}Pu/^{239}Pu$	-	0.172 ±0.001	Pu fraction
^{238}Pu	4.1 ± 0.4	-	Pu fraction
^{242}Pu	2.2 ± 0.3	-	Pu fraction
$^{237}Np/^{239}Pu$	-	3,41E+00 ± 5,14E-01 4,06E-03 ± 6,69E-05 8,64E-02 ± 1,87E-02	U fraction Pu fraction X fraction
^{241}Am	4.3 ± 0.2	-	Th fraction
$^{243}Am/^{241}Am$	-	2.97E-02 ± 2.97E-02	Th fraction
^{137}Cs	25926 ± 1715		

4.1.2 Cryo. 7

Nuclide	Bq/kg estimated	Ratio	Comment
^{238}U	11.6 ± 0.2 0.3 ± 0.05	-	U fraction X faction
$^{236}U/^{238}U$	-	1.46E-06 ± 1.50E-07 3.53E-05 ± 1.90E-06	U fraction X fraction
^{234}U	12.2 ± 0.2	-	U fraction
$^{234}U/^{238}U$	-	5,57E-05 5,42E-05	U fraction X fraction
^{232}U	0.3 ± 0.04	-	U fraction
$^{239+240}Pu$	5.2 ± 0.2 36.2 ± 0.5	-	Pu fraction X fraction
$^{240}Pu/^{239}Pu$	0,174 ± 0.001	-	Pu fraction
^{238}Pu	0.7± 0.08	-	Found in Pu fraction
^{242}Pu	-	-	
$^{237}Np/^{239}Pu$	-	1,59E-01 ± 2,13E-02 1,66E-03 ± 2,35E-03 3,95E-03 ± 5,61E-03	U fraction Pu fraction X fraction
^{241}Am	5.0 ± 0.3		Th fraction
$^{243}Am/^{241}Am$		4.88E-02 ± 4.88E-02	Th fraction
^{137}Cs	103429 ± 8164		

4.1.3 Cryo 9

Nuclide	Bq/kg estimated	Ratio	Comment
^{238}U	20.6 ± 0.6 0.9 ± 0.1	-	U fraction X fraction
$^{236}U/^{238}U$	-	1.10E-05 ± 6.00E-08 5.36E-05 ± 1.90E-06	U fraction X fraction
^{234}U	21.4 ± 0.6 1.3 ± 0.1	-	U fraction X fraction
$^{234}U/^{238}U$	-	5,87E-05 4,31E-05	U fraction X fraction
^{232}U	1.5 ± 0.1	-	U fraction
$^{239+240}Pu$	51.6 ± 1.8 18.4 ± 0.2	-	Pu fraction X fraction
$^{240}Pu/^{239}Pu$	-	0,174 ± 0,001	Pu fraction
^{238}Pu	1.5 ± 0.3	-	Pu fraction
^{242}Pu	-	-	
$^{237}Np/^{239}Pu$	-	2,15E+00 ± 1,45E-01 4,35E-03 ± 1,41E-04 7,67E-02 ± 2,86E-03	U fraction Pu fraction X fraction
^{241}Am	7.0 ± 0.4	-	Th fraction
$^{243}Am/^{241}Am$	-	-	
^{137}Cs	20006 ± 1542	-	

4.1.4 Cryo 11

Nuclide	Bq/kg estimated	Ratio	Comment
^{238}U	9.2 ± 0.3 3.4 ± 0.1	-	U fraction X fraction
$^{236}U/^{238}U$	-	4.33E-06 ± 2.00E-07 1.07E-05 ± 1.60E-07	U fraction X fraction
^{234}U	9.9 ± 0.3 3.8 ± 0.1	-	U fraction X fraction
$^{234}U/^{238}U$	-	6,21E-05 1,18E-05	U fraction X fraction
^{232}U	1.1 ± 0.1	-	U fraction
$^{239+240}Pu$	7.6 ± 0.2 39.7 ± 1.0	-	Pu fraction X fraction
$^{240}Pu/^{239}Pu$	-	0,184 ± 0,016	Pu fraction
^{238}Pu	0.9 ± 0.08	-	Pu fraction
^{242}Pu	-	-	
$^{237}Np/^{239}Pu$	-	3,47E-01 ± 4,21E-02 0,00E+00 ± 6,51E-04 8,13E-03 ± 3,08E-03	U fraction Pu fraction X fraction
^{241}Am	4.1 ± 0.2	-	Th fraction
$^{243}Am/^{241}Am$	-	-	
^{137}Cs	81150 ± 6186	-	

4.1.5 Blank

Nuclide	Bq/Sample estimated	Ratio	Comment
^{238}U	0.00072 ± 9.182E-05 0.00243 ± 0.000314	-	U fraction Th fraction
$^{236}U/^{238}U$	-	1.22E-05 ± 2.50E-07 4.14E-06 ± 1.80E-07	U fraction X fraction
^{234}U	0.00102 ± 0.000118 0.00255 ± 0.000314	-	U fraction Th fraction
$^{234}U/^{238}U$	-	-	
^{232}U	0.00013 ± 3.935E-05	-	U fraction
$^{239+240}Pu$	0.00055 ± 7.869E-05	-	Pu fraction
$^{240}Pu/^{239}Pu$	-	0,026 ± 0,010	Pu fraction
^{238}Pu	0.00055 ± 7.869E-05	-	Pu fraction
^{242}Pu	-	-	
$^{237}Np/^{239}Pu$	-	1,28E-02 ± 5,48E-03 2,80E-03 ± 3,97E-03 4,08E-03 ± 3,55E-03	U fraction Pu fraction X fraction

4.1.6 ALMERA SOIL 1 IAEA 0375

Nuclide	Literature	Ratio	Comment
$^{240}Pu/^{239}Pu$	0,18 (+/- 0,03)[40] 0,22 (+/- 0,01)[39]	0,210 ± 0,011	Pu fraction
$^{237}Np/^{239}Pu$	-	6,08E-02 ± 4,18E-03	Pu fraction

4.2 Sample preparation with spike (for alpha spectrometry)

4.2.1 Cryo. 3

Nuclide	Bq/kg calculated	Comment
^{238}U	25.6 ± 2.3 11.9 ± 1.3	U fraction Residue from U fraction
^{234}U	26.8 ± 1.3 14.9 ± 4.1	U fraction Residue from U fraction
$^{239+240}Pu$	75.1 ± 1.7	Pu fraction
^{238}Pu	2.7 ± 0.2	Pu fraction

4.2.2 Cryo. 7

Nuclide	Bq/kg calculated	Comment
^{238}U	17.0 ± 1.1	U fraction
^{234}U	18.5 ± 1.1	U fraction
$^{239+240}Pu$	8.7 ± 0.4 30.4 ± 1.3	Pu fraction X fraction
^{238}Pu	1.3 ± 0.1	Pu fraction

4.2.3 Cryo 9

Nuclide	Bq/kg calculated	Comment
^{238}U	25.8 ± 0.8	U fraction
^{234}U	27.7 ± 0.8	U fraction
$^{239+240}Pu$	195.7 ± 2.6	Pu fraction
^{238}Pu	4.7 ± 0.1	Pu fraction

4.2.4 Cryo 11

Nuclide	Bq/kg calculated	Comment
^{238}U	17.8 ± 1.8	U fraction
^{234}U	18.8 ± 1.4	U fraction
$^{239+240}Pu$	15.3 ± 0.8 3.6 ± 0.3	Pu fraction X fraction
^{238}Pu	15.3	Pu fraction

5. Discussion

5.1 ^{236}U and $^{236}U/^{238}U$ ratios

The Uranium blank was measured by Alpha spectroscopy and already here Uranium was visible, indicating a contamination. AMS showed a blank level for the $^{236}U/^{238}U$ atomic ratio of 1.22E-05 ± 2.50E-07. This level had been frequently measured in our lab before and indicates a contamination source inside the laboratory. Therefore a final conclusion about the exact $^{236}U/^{238}U$ atomic ratios is not possible at the moment. However, with the reported $^{236}U/^{239}Pu$ atomic ratios in [8] (highest value:14 in top soil)[8] and the calculated ^{239}Pu atomic numbers from the alpha spectroscopy data an estimation is possible. From the above given ratio the calculated value for the number of ^{236}U atoms/kg in Cryo9. would be in the order of E15 atoms. However, from our measured data ($^{239+240}Pu$: 195 Bq/kg; $^{240}Pu/^{239}Pu$: 0,174; ^{238}U: 25 Bq/kg; $^{236}U/^{238}U$: 1.0E-5) the number of ^{236}U atoms/kg is only in the order of E13, two orders of magnitude lower than expected. This leads to the conclusion that due to its higher water solubility compared to plutonium, uranium has been washed out from the cryoconites.

5.2 $^{234}U/^{238}U$ ratios

The $^{234}U/^{238}U$ ratios are in the expected range of E-5 which is the common ratio for environmental samples given the natural abundance distribution of Uranium isotpes (Chapter 1.1). The measured activity concentrations between 17 and 25 mBq/g correspond to 1.4 - 2.0 µg/g (ppm). This is a value usually found for soil samples and indicates resuspended matter as part of the inorganic components of cryoconites (the (here not given) ^{232}Th activity concentrations support this assumption).

5.3 $^{239+240}Pu$, ^{238}Pu and $^{240}Pu/^{239}Pu$ ratios

The comparison of our $^{239+240}Pu$ and ^{238}Pu data with data from [18] showed good agreement (deviations from 0.3% up to 10%). This also allows the conclusion that our method with the cheaper ion exchange resin can be used.

The absence of H_3BO_3 in the spiked procedure of Cryo3. shows a significant difference in activity concentration of $^{239+240}Pu$ with 75.1 ± 1.7 Bq/kg in the sample of this thesis compared to 164.6 ± 6.6 Bq/kg in the sample of [18]. This shows that a significant amount of the nuclides is enclosed in silicates.

The analysis of the X fractions in the spiked procedure showed additional $^{239+240}Pu$,but no ^{242}Pu-spike in Cryo 11. and Cryo 7. With an activity concentration of 8.7 ± 0.4 Bq/kg in the Pu fraction and 30.4 ± 1.3 Bq/kg in the X fraction of the sample Cryo7. the total activity concentration is more than 4 times higher than the published value. This indicates that a deeper analysis of the separation and pretreatment steps is necessary in order to allow an appropriate measurement of Plutonium which is known for its complex chemistry (Chapter 1.2). The $^{240}Pu/^{239}Pu$ ratios found in the samples range from 0.172 ±0.001 to 0,184 ± 0,016 indicating global fallout (Chapter 1.2). However, already Tieber et al. pointed out that Pu from Chernobyl fallout quite sure is also present but its relatively low amount is superimposed by global fallout.[18]

5.3 ^{237}Np

The first step for the analysis of ^{237}Np in cryoconites can be seen successful and showed interesting facts for future analysis. With a measured ratio of 3,41E+00 ± 5,14E-01 for $^{237}Np/^{239}Pu$ in Cryo 3. and 2,15E+00 ± 1,45E-01 in Cryo 9 both are far above the reported ratios in [38]. The AMS data showed the main portions of ^{237}Np in the U fraction and Pu fraction. For further analysis a method has to be found which allows separation in to a single fraction.

5.4 ^{243}Am and ^{241}Am

^{241}Am was found in the Th fraction but overlapping with the ^{228}Th peak which made an appropriate evaluation from the alpha spectrum impossible. This fact is also reflected in the measured ^{241}Am activity concentration for Cryo3. and Cryo9. which is only about 5% and 10%, respectively, of the published data in [18]. For a further analysis with alpha spectroscopy a method has to applied which allows the separation of Thorium and

Americium. The measured atomic ratio for $^{243}Am/^{241}Am$ in Cryo3. (2.97E-02 ± 2.97E-02) is only a very rough estimation due to the large uncertainty.

5.4 ^{137}Cs

A good correlation between our ^{137}Cs data and the data from [18] was found with the biggest deviation being 7%.

6. Summary

Cryoconite samples for this master thesis were provided by the University of Salzburg and had been collected at the Hallstätter and Schladming glacier in the Northern Calcareous Alps in Upper Austria. Cryoconites are airborne sediments deposited on a glacier and can be seen as rather pure fallout containing high amounts of anthropogenic radionuclides. The possibility of using Alpha and Gamma spectroscopy as well as Accelerator Mass Spectroscopy allowed to measure also actinides at ultra-low levels as well as to determine isotopic ratios not accessible by Alpha Spectrometry.

The measurement of ^{137}Cs and $^{239+240}$Pu activity concentrations in the samples corresponded well with already published data with a range from 20 to 103 kBq/kg and 15 to 195 Bq/kg, respectively. However, additional $^{239+240}$Pu was found in the so-called X-fraction of the separation, demonstrating the fact that different Pu species could not be “unified” in the sample pre-treatment step. In one case the activity in the X-fraction was 3.5 times higher than the published value in [18] for the respective sample (30.4 Bq/kg compared to 8.7 Bq/kg). The ^{240}Pu/^{239}Pu ratios found in the samples range from 0.17 to 0.18 indicating global fallout as the main source of Pu.

Due to the high blank levels, ^{236}U/^{238}U ratios could not be measured properly. This was surprising, as from the ^{236}U/^{239}Pu atomic ratios for global fallout given in the literature much higher amounts of ^{236}U were expected.

For Am and Np no separation steps were performed in this first run, so all fractions were checked for these nuclides by AMS. ^{241}Am was found in the Th-fraction but could not be quantified due to lack of spike. It was however possible to see ^{237}Np in Austrian samples for the first time. ^{237}Np was found in the U- as well as in the Pu-fractions. In future studies it must be assured that all Np is in the Pu-fraction in order to be able to calculate reliable ^{237}Np/^{239}Pu ratios.

7. Literature

[1] E.Riedel, C.Janiak, *Anorganische Chemie*, **2007**, de Gruyter, Berlin

[2] K.J.R. Rosman, P.D.P. Taylor, *Pure Appl. Chem.*, **1999**, 71, 1593-1607

[3] J. Magill, G. Pfennig, R. Dreher, Z. Sóti, *Chart of Nuclides, 9th Edition*, **2015**

[4] F. Monroy-Guzmán, *J. Chem. Chem. Eng.* **2016**, 10, 90-95

[5] S. De Houwer, C. Görller-Walrand, *Journal of Alloys and Compounds,* **2001** 323–324, 683–687

[6] F. Quinto, E. Hrnecek, M. Krachler, W. Shotyk, P. Steier, S.R. Winkler, **2013**, *Environmental Science&Technology,* 47, 5243-5250;

[7] W. Stephan, P. Steier, J. Carilli, **2012,** *Earth and Planet. Sci. Lett. 359-360: 124–130;*

[8] F. Quinto, E. Hrnecek, M. Krachler, W. Shotyk, P. Steier,St. R. Winkler, *Environ. Sci. Technol.* **2013**, 47, 5243-5250

[9] P.Steier, M.Bichler, L.K. Fifield, R. Golser, W. Kutschera, A. Priller, F. Quinto, S. Richter, M. Srncik, P. Terrasi, L. Wacker, A. Wallner, G. Wallner, K.M. Wilcken, E.M. Wild, *Nucl. Instrum. Methods Phys. Res. Sect. B***, 2008**, 226, 2246-2250

[10] S.F. Boulyga, J.S. Becker, *Fresenius J. Anal. Chem*. **2001**, 370, 612-617

[11] V.P. Mironov, J.L. Matusevich, V.P. Kudrjashov, S.F. Boulyga, J.S. Becker, J. Environ. Monit. **2002**, 4, 997-1002

[12] O.J. Marsden, F.R. Livens, J.P. Day, L.K. Fifield, P.S. Goodall, *Analyst,* **2001**, 126, 633-636

[13] P.Jannasch, O. Heidenreich, *Zeitschrift für Anorganische Chemie,* **1896,** 12, 1, 208-218

[14] N. Takeuchi, S. Kohshima, K. Seko,*Arctic, Antarctic, and Alpine Research*, **2001**, 33, 2,115-122

[15] http://www-es.s.chiba-u.ac.jp/~takeuchi/cryoconite.html

[16] http://www-es.s.chiba-u.ac.jp/~takeuchi/crygranule.html

[17] E. Łokas, A. Zaborska, M. Kolicka, M. Rózycki,K. Zawierucha, *Chemosphere,* **2016**, 100, 162-172

[18] A. Tieber, H. Lettner, P. Bossew, A. Hubmer, B. Sattler, W. Hofmann, *Journal of Environmental Radioactivity,* **2009**, 100, 590 - 598

[19] *UNSCEAR 2008 Report. Sources and effects of ionizing radiation*. Band 2. *Annex D – Health effects due to radiation from the Chernobyl accident*. New York 2011, S. 49

[20] N.Vajda,C.-K. Kim, *J. Radioanal. Nucl. Chem.* **2010,** 284, 341-366.

[21] https://www.inorganicventures.com/ashing-sample-preparation-procedures

[22] http://www.sigmaaldrich.com/catalog/product/sial/217387?lang=de&region=AT

[23] J.Krtil, J.Mencl, A.Moravec*, Radiochem. Radioanal. Lett.* **1975** 21(3-4), 115-120

[24] N.Vajda,C.-K. Kim, *Journal of Radioanalytical and Nuclear Chemistry*, **2010**, 283,1,203-223

[25] C.Vockenhuber, R.Golser, W.Kutschera W., A.Priller, P.Steier, S. Winkler, V.Liechtenstein, *Pramana-J. Phys.* **2002**, 59(6), 1041-1051

[26] P.Steier, R.Golser, W. Kutschera, A. Priller, C.Vockenhuber, S.Winkler, *Nucl. Instrum. Methods Phys. Res. Sect. B* **2004**, 223-224, 67-71.

[27] A. Krestou, D. Panias, *The European Journal of Mineral Processing and Environmental Protection,* **2004,** Vol.4, No.2, 1303-0868, 113-129

[28] Journal of Radioanalytical and Nuclear Chemistry, Articles, VoL 115, No. 2 (1987) 263-288

[29] J. Eberth, J. Simpson, *Progress in Particle and Nuclear Physics*, **2008**, 60, 283–337

[30] P.Steier, F.Dellinger, O. Forstner, R. Golser, K. Knie, W. Kutschera, A. Priller, F.Quinto, M. Srncik, F.Terrasi, C.Vockenhuber, A. Wallner, G. Wallner, E.M. Wild, *Nucl.Instrum. Methods Phys. Res., Sect. B,* **2010**, 268, 1045-1049

[31] K.H. Purser, L. R. Kilius., A. E. Litherland, X. Zhao, *Nuclear Instruments and Methods in Physics Research Section B*, **1996,** 113, 1-4, 445-452

[32] S.Richter, A. Alonso, W. De Bolle, R. Wellum, P.D.P. Taylor, *Int. J. Mass Spectrom.* **1999**, 193, 9-14.

[33] C.F.Metz, *Analytical Chemistry,* **1957,** (29) 12, 1748-1756

[34] A. F. Holleman, E. Wiberg, N. Wiberg: *Lehrbuch der Anorganischen Chemie,* **2007**, Gruyter, Berlin

[35] P.Lindahl, P.Roos, E.Holm, E.Dahlgaard, *Journal of Environmental Radioactivity,* **2005**, 82,285-301

[36] F.Quinto, E.Hrnecek , M.Krachler , W.Shotyk , P.Steier , SR.Winkler*, Environ. Sci.Process Impacts*, **2013**, 4, 839-847

[37] S.Salminen-Paatero, U.Nygren, J. Paatero, *Journal of Environmental Radioactivity,* **2012,** 113, 163-170

[38] T.M.Beasley, J.M.Kelley, T.C.Maiti, L.A.Bond, *Journal of Environmental Radioactivity,***1998**, 38, 2, 133-146

[39] C.S. Kim, C.K.Kim,J.I. Lee, K.J. Lee, *Journal of Analytical Atomic Spectrometry,* **2000**, 15, 247-255

[40] J.Qiao, V.Hansen, X.Hou, A.Aldahan,G.Possnert, *Applied Radiation and Isotopes,* **2012,** 70, 8, 1698-1708

[41] *S.*Cotton*, Lanthanides and Actinides*, **1991**, New York: Oxford University Press

8. Appendix

8.1 Gamma spectroscopy data for samples prepared without spike

For the calculation of the detector efficency a reference sample of ^{137}Cs was used (A =26467 Bq Jan. 2017). With 14339 counts in 62 s, the calculated detector efficeny is 4.84%. The emission probability for a gamma quant/decay is 0.84.

Sample	Amount (g)	Counts	Error	Time (s)	Detector and emission corr. Counts/s(Bq)	Error	Bq/kg	Error(1σ)	Ratio MB/[18]
Cryo 3.	0.20	2667	56	70073	5.2	0.3	25926	1715	1.03
Cryo 7.	0.23	901	33	5160	23.8	1.9	10342 9	8164	0.93
Cryo 9.	0.25	1022	35	27838	5.0	0.4	20006	1542	1.01
Cryo 11.	0.19	1085	36	9587	15.4	1.2	81150	6186	1.07

8.2. Alpha spectroscopy data for samples prepared without spike

Cryo 3.	238U	Integral	Error(1σ)	Time(s)	Bq/Sample	Bq/kg	Error(1σ)
0.5g							
	U Fraction	753	24	346459	0.0072	14.4	0.4
	Pu Fraction						
	Th Fraction						
	X Fraction	56	7	342920	0.00054	1.0	0.1
Cryo 3.	234U	Integral	Error(1σ)	Time(s)	Bq/Sample	Bq/kg	Error(1σ)
0.5g							
	U Fraction	877	29	346459	0.0084	16.8	0.5
	Pu Fraction						
	Th Fraction						
	X Fraction	84	9	342920	0.00081	1.6	0.1
Cryo 3.	232U	Integral	Error(1σ)	Time(s)	Bq/Sample	Bq/kg	Error(1σ)
0.5g							
	U Fraction	44	6	346459	0.00042	0.8	0.1
	Pu Fraction						
	Th Fraction						
	X Fraction	488	22	342920	0.00474	9.4	0.4
Cryo 3.	239+240Pu	Integral	Error(1σ)	Time(s)	Bq/Sample	Bq/kg	Error(1σ)
0.5g							
	U Fraction						
	Pu Fraction	2671	51	146080	0.06094	121.8	2.3
	Th Fraction						
	X Fraction						
Cryo 3.	238Pu	Integral	Error(1σ)	Time(s)	Bq/Sample	Bq/kg	Error(1σ)
0.5g							
	U Fraction						
	Pu Fraction	92	9	146080	0.00209	4.1	0.4
	Th Fraction						
	X Fraction						

Cryo 3.	241Am	Integral	Error(1σ)	Time(s)	Bq/Sample	Bq/kg	Error(1σ)
0.5g							
	U Fraction						
	Pu Fraction						
	Th Fraction	222	15	343281	0.00215	4.3	0.2
	X Fraction						

Cryo 3.	242Pu	Integral	Error(1σ)	Time(s)	Bq/Sample	Bq/kg	Error(1σ)
0.5g							
	U Fraction						
	Pu Fraction	50	7	146080	0.00114	2.2	0.3
	Th Fraction						
	X Fraction						

Cryo 7.	238U	Integral	Error(1σ)	Time(s)	Bq/Sample	Bq/kg	Error(1σ)
1.3g							
	U Fraction	1528	39	335808	0.01516	11.6	0.2
	Pu Fraction	30	5	250117	0.00039	0.3	0.05
	Th Fraction						
	X Fraction						

Cryo 7.	234U	Integral	Error(1σ)	Time(s)	Bq/Sample	Bq/kg	Error(1σ)
1.3g							
	U Fraction	1599	39	335808	0.01587	12.2	0.2
	Pu Fraction						
	Th Fraction						
	X Fraction						

Cryo 7.	232U	Integral	Error(1σ)	Time(s)	Bq/Sample	Bq/kg	Error(1σ)
1.3g							
	U Fraction	41	6	335808	0.00040	0.3	0.04
	Pu Fraction						
	Th Fraction						
	X Fraction						

Cryo 7.	239+240Pu	Integral	Error(1σ)	Time(s)	Bq/Sample	Bq/kg	Error(1σ)
1.3g							
	U Fraction						
	Pu Fraction	515	22	250117	0.00686	5.2	0.2
	Th Fraction						
	X Fraction	4742	69	335870	0.04706	36.2	0.5

Cryo 7.	238Pu	Integral	Error(1σ)	Time(s)	Bq/Sample	Bq/kg	Error(1σ)
1.3g							
	U Fraction						
	Pu Fraction	74	8	250117	0.00098	0.3	0.08
	Th Fraction						
	X Fraction						
Cryo 7.	241Am	Integral	Error(1σ)	Time(s)	Bq/Sample	Bq/kg	Error(1σ)
1.3g							
	U Fraction						
	Pu Fraction						
	Th Fraction	201	14	102000	0.00656	5.0	0.3
	X Fraction	-					
Cryo 7.	242Pu	Integral	Error(1σ)	Time(s)	Bq/Sample	Bq/kg	Error(1σ)
1.3g							
	U Fraction						
	Pu Fraction						
	Th Fraction						
	X Fraction						

Cryo 9.	238U	Integral	Error(1σ)	Time(s)	Bq/Sample	Bq/kg	Error(1σ)
0.5g							
	U Fraction	1037	32	334414	0.01033	20.6	0.6
	Pu Fraction						
	Th Fraction						
	X Fraction	39	6	260747	0.00049	0.9	0.1
Cryo 9.	234U	Integral	Error(1σ)	Time(s)	Bq/Sample	Bq/kg	Error(1σ)
0.5g							
	U Fraction	1076	33	334414	0.01072	21.4	0.6
	Pu Fraction						
	Th Fraction						
	X Fraction	53	7	260747	0.00067	1.3	0.1
Cryo 9.	232U	Integral	Error(1σ)	Time(s)	Bq/Sample	Bq/kg	Error(1σ)
0.5g							
	U Fraction	77	8	334414	0.00076751	1.5	0.1
	Pu Fraction						
	Th Fraction						
	X Fraction						

Cryo 9.	239+240Pu	Integral	Error(1σ)	Time(s)	Bq/Sample	Bq/kg	Error(1σ)
0.5g							
	U Fraction						
	Pu Fraction	787	28	101548	0.02583343	51.6	1.8
	Th Fraction						
	X Fraction	722	27	260747	0.0092298	18.4	0.2
Cryo 9.	238Pu	Integral	Error(1σ)	Time(s)	Bq/Sample	Bq/kg	Error(1σ)
0.5g							
	U Fraction						
	Pu Fraction	24	5	101548	0.0007878	1.5	0.3
	Th Fraction						
	X Fraction						
Cryo 9.	241Am	Integral	Error(1σ)	Time(s)	Bq/Sample	Bq/kg	Error(1σ)
0.5g							
	U Fraction						
	Pu Fraction						
	Th Fraction	275	16	261847	0.00350	7.0	0.4
	X Fraction						
Cryo 9.	242Pu	Integral	Error(1σ)	Time(s)	Bq/Sample	Bq/kg	Error(1σ)
0.5g							
	U Fraction						
	Pu Fraction						
	Th Fraction						
	X Fraction						

Cryo 11.	238U	Integral	Error(1σ)	Time(s)	Bq/Sample	Bq/kg	Error(1σ)
1.0g							
	U Fraction	690	26	248438	0.00925	9.2	0.3
	Pu Fraction	412	20	393360	0.00349	3.4	0.1
	Th Fraction						
	X Fraction						
Cryo 11.	234U	Integral	Error(1σ)	Time(s)	Bq/Sample	Bq/kg	Error(1σ)
1.0g							
	U Fraction	744	27	248438	0.00998	9.9	0.3
	Pu Fraction	460	21	393360	0.00389	3.8	0.1
	Th Fraction						
	X Fraction						

Cryo 11.	232U	Integral	Error(1σ)	Time(s)	Bq/Sample	Bq/kg	Error(1σ)
1.0g							
	U Fraction	82	9	248438	0.00110	1.1	0.1
	Pu Fraction						
	Th Fraction						
	X Fraction						
Cryo 11.	239+240Pu	Integral	Error(1σ)	Time(s)	Bq/Sample	Bq/kg	Error(1σ)
1.0g							
	U Fraction						
	Pu Fraction	901	30	393360	0.00763	7.6	0.2
	Th Fraction						
	X Fraction	1475	38	121893	0.04033	39.7	1.0
Cryo 11.	238Pu	Integral	Error(1σ)	Time(s)	Bq/Sample	Bq/kg	Error(1σ)
1.0g							
	U Fraction						
	Pu Fraction	108	10	393360	0.00091	0.9	0.08
	Th Fraction						
	X Fraction						
Cryo 11.	241Am	Integral	Error(1σ)	Time(s)	Bq/Sample	Bq/kg	Error(1σ)
1.0g							
	U Fraction						
	Pu Fraction						
	Th Fraction	277	16	223261	0.00413	4.1	0.2
	X Fraction						
Cryo 11.	242Pu	Integral	Error(1σ)	Time(s)	Bq/Sample	Bq/kg	Error(1σ)
1.0g							
	U Fraction						
	Pu Fraction						
	Th Fraction						
	X Fraction						

Blank	238U	Integral	Error(1σ)	Time(s)	Bq/Sample	Error(1σ)
	U Fraction	55	7	254132	0.00072	9.182E-05
	Pu Fraction					
	Th Fraction	62	8	84935	0.00243	0.000314
	X Fraction					

Blank	234U	Integral	Error(1σ)	Time(s)	Bq/Sample	Error(1σ)
	U Fraction	78	9	254132	0.00102	0.000118
	Pu Fraction					
	Th Fraction	65	8	84935	0.00255	0.000314
	X Fraction					
Blank	232U	Integral	Error(1σ)	Time(s)	Bq/Sample	Error(1σ)
	U Fraction	10	3	254132	0.00013	3.935E-05
	Pu Fraction					
	Th Fraction					
	X Fraction					
Blank	239+240Pu	Integral	Error(1σ)	Time(s)	Bq/Sample	Error(1σ)
	U Fraction					
	Pu Fraction	42	6	254162	0.00055	7.869E-05
	Th Fraction					
	X Fraction					
Blank	238Pu	Integral	Error(1σ)	Time(s)	Bq/Sample	Error(1σ)
	U Fraction					
	Pu Fraction	42	6	254162	0.00055	7.869E-05
	Th Fraction					
	X Fraction					
Blank	241Am	Integral	Error(1σ)	Time(s)	Bq/Sample	Error(1σ)
	U Fraction					
	Pu Fraction					
	Th Fraction					
	X Fraction					
Blank	242Pu	Integral	Error(1σ)	Time(s)	Bq/Sample	Error(1σ)
	U Fraction					
	Pu Fraction					
	Th Fraction					
	X Fraction					

8.3. Alpha spectroscopy data for samples prepared with spike

Cryo 3.	238U	Integral	Counts/s	Error	Error/s	Time(s)	Bq/kg	Error(1σ)	Yield
0.2g ^{242}Pu spike 14.4 mBq ^{232}U spike 17.7 ± 0.9 mBq	U Fraction	272	0.000544	16	0.000032	500000	25.6	2.3	
	Pu Fraction								
	Residue from U Fraction	126	0.000252	11	0.000022	500000	11.9	1.35	
Cryo 3.	234U	Integral	Counts/s	Error	Error/s	Time(s)	Bq/kg	Error(1σ)	Yield
0.2g ^{242}Pu spike 14.4 mBq ^{232}U spike 17.7 ± 0.9 mBq	U Fraction	285	0.000570	17	0.000034	500000	26.8	1.3	
	Pu Fraction								
	Residue from U Fraction	158	0.000316	13	0.000026	500000	14.9	4.1	
Cryo 3.	232U	Integral	Counts/s	Error	Error/s	Time(s)	Bq/kg	Error(1σ)	Yield
0.2g ^{242}Pu spike 14.4 mBq ^{232}U spike 17.7 ± 0.9 mBq	U Fraction	661	0.001322	28	0.000056	500000	---		35.4%
	Pu Fraction								
	Residue from U Fraction	279	0.000558	17	0.000034	500000	---		
Cryo 3.	239+240Pu	Integral	Counts/s	Error	Error/s	Time(s)	Bq/kg	Error(1σ)	Yield
0.2g ^{242}Pu spike 14.4 mBq ^{232}U spike 17.7 ± 0.9 mBq	U Fraction								
	Pu Fraction	3582	0.007164	60	0.00012	500000	75.1	1.7	
	Residue from U Fraction								

Cryo 3.	238Pu	Integral	Counts/s	Error	Error/s	Time(s)	Bq/kg	Error(1σ)	Yield
0.2g ^{242}Pu spike 14.4 mBq ^{232}U spike 17.7 ± 0.9 mBq	U Fraction								
	Pu Fraction	129	0.000258	11	0.000022	500000	2.7	0.2	
	Residue from U Fraction								
Cryo 3.	242Pu	Integral	Counts/s	Error	Error/s	Time(s)	Bq/kg	Error(1σ)	Yield
0.2g ^{242}Pu spike 14.4 mBq ^{232}U spike 17.7 ± 0.9 mBq	U Fraction								
	Pu Fraction	3435	0.006870	58.60887305	0.000117	500000	----		
	Residue from U Fraction								
Cryo 7.	238U	Integral	Counts/s	Error	Error/s	Time(s)	Bq/kg	Error(1σ)	Yield
1.0g 242Pu spike 14.4 mBq 232U spike 17.7 ± 0.9 mBq	U Fraction	1224	0.003417	34	9.7E-05	358207	17.0	1.1	
	Pu Fraction								
	Th Fraction								
	X Fraction								
Cryo 7.	234U	Integral	Counts/s	Error	Error/s	Time(s)	Bq/kg	Error(1σ)	Yield
1.0g 242Pu spike 14.4 mBq 232U spike 17.7 ± 0.9 mBq	U Fraction	1334	0.003724	36	0.000101	358207	18.5	1.1	
	Pu Fraction								
	Th Fraction								
	X Fraction								

Cryo 7.	232U	Integral	Counts/s	Error	Error/s	Time(s)	Bq/kg	Error(1σ)	Yield
									67.0%
1.0g 242Pu spike 14.4 mBq 232U spike 17.7 ± 0.9 mBq	U Fraction	1276	0.003562	35	9.9E-05	358207	----		
	Pu Fraction								
	Th Fraction								
	X Fraction								
Cryo 7.	239+240Pu	Integral	Counts/s	Error	Error/s	Time(s)	Bq/kg	Error(1σ)	Yield
1.0g 242Pu spike 14.4 mBq 232U spike 17.7 ± 0.9 mBq	U Fraction								
	Pu Fraction	528	0.001589	22	6.9E-05	332348	8.7	0.4	
	Th Fraction								
	X Fraction	1409	0.005569	37	0.000148	252990	30.4	1.3	
Cryo 7.	238Pu	Integral	Counts/s	Error	Error/s	Time(s)	Bq/kg	Error(1σ)	Yield
1.0g 242Pu spike 14.4 mBq 232U spike 17.7 ± 0.9 mBq	U Fraction								
	Pu Fraction	77	0.000232	8	2.6E-05	332348	1.3	0.1	
	Th Fraction								
	X Fraction								
Cryo 7.	242Pu	Integral	Counts/s	Error	Error/s	Time(s)	Bq/kg	Error(1σ)	Yield
									61.1%
1.0g 242Pu spike 14.4 mBq 232U spike 17.7 ± 0.9 mBq	U Fraction								
	Pu Fraction	878	0.002642	29	8.9E-05	332348	-----		
	Th Fraction								
	X Fraction								

Cryo 9.	238U	Integral	Counts/s	Error	Error/s	Time(s)	Bq/kg	Error(1σ)	Yield
0.5g ^{242}Pu spike 14.4 mBq ^{232}U spike 17.7 ± 0.9 mBq	U Fraction	1159	0.002692	34	7.94E-05	430505	25.8	0.8	
	Pu Fraction								
	Th Fraction								
	X Fraction								
Cryo 9.	234U	Integral	Counts/s	Error	Error/s	Time(s)	Bq/kg	Error(1σ)	Yield
0.5g ^{242}Pu spike 14.4 mBq ^{232}U spike 17.7 ± 0.9 mBq	U Fraction	1246	0.002894	34	8.1E-05	430505	27.7	0.8	
	Pu Fraction								
	Th Fraction								
	X Fraction								
Cryo 9.	232U	Integral	Counts/s	Error	Error/s	Time(s)	Bq/kg	Error(1σ)	Yield
0.5g ^{242}Pu spike 14.4 mBq ^{232}U spike 17.7 ± 0.9 mBq	U Fraction	1593	0.003700	39	9.2E-05	430505	----		69.6%
	Pu Fraction								
	Th Fraction								
	X Fraction								
Cryo 9.	239+240Pu	Integral	Counts/s	Error	Error/s	Time(s)	Bq/kg	Error(1σ)	Yield
0.5g ^{242}Pu spike 14.4 mBq ^{232}U spike 17.7 ± 0.9 mBq	U Fraction								
	Pu Fraction	10565	0.023743	102	0.00023	444970	195.7	2.6	
	Th Fraction								
	X Fraction								

Cryo 9.	238Pu	Integral	Counts/s	Error	Error/s	Time(s)	Bq/kg	Error(1σ)	Yield
0.5g ^{242}Pu spike 14.4 mBq ^{232}U spike 17.7 ± 0.9 mBq	U Fraction								
	Pu Fraction	256	0.000575	16	3.5E-05	444970	4.7	0.1	
	Th Fraction								
	X Fraction								

Cryo 9.	242Pu	Integral	Counts/s	Error	Error/s	Time(s)	Bq/kg	Error(1σ)	Yield
0.5g ^{242}Pu spike 14.4 mBq ^{232}U spike 17.7 ± 0.9 mBq	U Fraction								80.8%
	Pu Fraction	1555	0.003495	39	8.8E-05	444970	-----		
	Th Fraction								
	X Fraction								

Cryo 11.	238U	Integral	Counts/s	Error	Error/s	Time(s)	Bq/kg	Error(1σ)	Yield
1.0g ^{242}Pu spike 14.4 mBq ^{232}U spike 17.7 ± 0.9 mBq	U Fraction	575	0.003863	23	0.000161	148836	17.8	1.8	
	Pu Fraction								
	Th Fraction								
	X Fraction								

Cryo 11.	234U	Integral	Counts/s	Error	Error/s	Time(s)	Bq/kg	Error(1σ)	Yield
1.0g ^{242}Pu spike 14.4 mBq ^{232}U spike 17.7 ± 0.9 mBq	U Fraction	608	0.004085	24	0.000165	148836	18.8	1.4	
	Pu Fraction								
	Th Fraction								
	X Fraction								

Cryo 11.	232U	Integral	Counts/s	Error	Error/s	Time(s)	Bq/kg	Error(1σ)	Yield
1.0g ^{242}Pu spike 14.4 mBq ^{232}U spike 17.7 ± 0.9 mBq									72.5%
	U Fraction	573	0.003850	23	0.000160	148836	-----		
	Pu Fraction								
	Th Fraction								
	X Fraction								
Cryo 11.	239+240Pu	Integral	Counts/s	Error	Error/s	Time(s)	Bq/kg	Error(1σ)	Yield
1.0g ^{242}Pu spike 14.4 mBq ^{232}U spike 17.7 ± 0.9 mBq									
	U Fraction								
	Pu Fraction	730	0.003094	27	0.000114	235929	15.3	0.8	
	Th Fraction								
	X Fraction	104	0.000730	10	7.1E-05	142464	3.6	0.3	
Cryo 11.	238Pu	Integral	Counts/s	Error	Error/s	Time(s)	Bq/kg	Error(1σ)	Yield
1.0g ^{242}Pu spike 14.4 mBq ^{232}U spike 17.7 ± 0.9 mBq									
	U Fraction								
	Pu Fraction	58	0.000246	7	3.29E-05	235929	1.2	0.1	
	Th Fraction								
	X Fraction								
Cryo 11.	242Pu	Integral	Counts/s	Error	Error/s	Time(s)	Bq/kg	Error(1σ)	Yield
1.0g ^{242}Pu spike 14.4 mBq ^{232}U spike 17.7 ± 0.9 mBq									67.3%
	U Fraction								
	Pu Fraction	686	0.002908	26	0.000111	235929	-----		
	Th Fraction								
	X Fraction								

8.4. AMS data for samples prepared without spike

	236U/ U238	Error	234U/ U238	240Pu/ 239Pu	Error	243Am/ 241Am	Error	237Np/ 239Pu	Error
Cryo3.U	8.03E-06	6.50E-08	5,36E-05					3,41E+00	5,14E-01
Cryo3.Pu				0,172	0,001			4,06E-03	6,69E-05
Cryo3.Th						2.97E-02	2.97E-02		
Cryo3.X	9.22E-06	3.30E-07	6,62E-05					8,64E-02	1,87E-02
Cryo7.U	1.46E-06	1.50E-07	5,57E-05					1,59E-01	2,13E-02
Cryo7.Pu				0,195	0,027			1,66E-03	2,35E-03
Cryo7.Th						4.88E-02	4.88E-02		
Cryo7.X	3.53E-05	1.90E-06	5,42E-05					3,95E-03	5,61E-03
Cryo9.U	1.10E-05	6.00E-08	5,87E-05					2,15E+00	1,45E-01
Cryo9.Pu				0,174	0,001			4,35E-03	1,41E-04
Cryo9.Th									
Cryo9.X	5.36E-05	1.90E-06	4,31E-05					7,67E-02	2,86E-03
Cryo11.U	4.33E-06	2.00E-07	6,21E-05					3,47E-01	4,21E-02
Cryo11.Pu				0,184	0,016			0,00E+00	6,51E-04
Cryo11.Th									
Cryo11.X	1.07E-05	1.60E-07	1,18E-05					8,13E-03	3,08E-03
Blank U	1.22E-05	2.50E-07						1,28E-02	5,48E-03
Blank X	4.14E-06	1.80E-07						2,80E-03	3,97E-03
Blank Pu				0,026	0,010			4,08E-03	3,55E-03
ALMERA SOIL 1 IAEA 0375				0,210	0,011			6,08E-02	4,18E-03

8.5 Abstract

This thesis deals with the activity concentration measurement of actinides in cryoconites from the Austrian Alps. These strongly homogeneous environmental samples containing biological, organic and inorganic compounds are found on the surface of glaciers. Its inorganic fraction are airborne sediments which transport natural as well as anthropogenic radionuclides to the glacier. In comparison to other environmental samples these cryoconites are rather 'pure' fallout samples and can therefore contain high concentrations of radionuclides.

^{137}Cs activity concentrations were measured by gamma spectroscopy, uranium and plutonium isotopes were separated from the matrix and from each other by ion exchange procedures and then measured by alpha spectrometry. Afterwards these samples were reprocessed and ^{236}U/^{238}U and ^{240}Pu/^{239}Pu atomic ratios were measured by Accelerator Mass Spectrometry (AMS).

Corresponding to already published data for these samples the ^{137}Cs activity concentrations are high (20 – 103 kBq/kg), $^{239+240}$Pu activity concentrations range from 15 – 195 Bq/kg. Atomic ratios of ^{240}Pu/^{239}Pu (0.17-0.18) indicate its origin from the global nuclear fallout. ^{236}U/^{238}U atomic ratios were surprisingly low (10^{-6}) but could not be interpreted due to our blank levels in the laboratory. With the highly sensitive AMS method also the occurrence of ^{237}Np could be verified in environmental samples in Austria for the first time.

8.6 Zusammenfassung

Thema dieser Arbeit war die Untersuchung der Aktivitätskonzentrationen von Aktiniden in Kryokoniten. Dieses Material welches auf Gletschern gefunden wird, enthält eine Vielzahl von biologischen, organischen und anorganischen Verbindungen. Einer der Grundstoffe für die Bildung dieses Materials sind windverfrachtete Aerosole, die unter anderem auch anthropogene Radionuklide beinhalten (allgemein bekannt unter der Bezeichnung Fallout). Die Matrix Gletscheroberfläche führt kaum zu Verdünnung der Aerosole mit anderen Materialen, das heißt, dass Kryokonitproben als beinahe reiner Fallout angesehen werden können. Dieser Umstand lässt stark erhöte Konzentrationen von Radionukliden in Kryokoniten erwarten.

Die Vielzahl an unterschiedlichen Nukliden und Zerfallsarten machte die Anwendung von mehreren chemischen und analytischen Methoden notwendig. Der Gammastrahler ^{137}Cs wurde mithilfe von Gammaspektrometrie gemessen. Uran und Plutonium wurden durch Ionenaustauscherharz getrennt und anschließend mittels Alphaspektrometrie quantifiziert. Diese Proben wurden anschließend für die Messung mit Accelerator Mass Spectrometry (AMS) aufbereitet um die Atomverhätlnisse $^{236}U/^{238}U$ und $^{240}Pu/^{239}Pu$ zu bestimmen.

Entsprechend der bereits publizierten Daten fanden wir hohe Aktivitätskonzentrationen von ^{137}Cs (20 – 103 kBq/kg). Die gefunden Aktivitätskonzentrationen von $^{239+240}Pu$ im Bereich von 15 – 195 Bq/kg stimmten ebenfalls mit den bereits bekannten Daten überein. Die erstmalig bestimmten $^{240}Pu/^{239}Pu$ Atomverhältnisse (0.17 – 0.18) entsprachen den Daten zu globalem Fallout. Die Atomverhältnisse von $^{236}U/^{238}U$ waren deutlich niedriger als erwartet (10^{-6}), konnten jedoch nicht weiter ausgewertet werden da die $^{236}U/^{238}U$ Verhältnisse der Blankproben zu hoch waren. Die Messung mit AMS ermöglichte auch den erstmalige Nachweis von ^{237}Np in österreichischen Umweltproben.